# JOURNAL OF ENGINEERING RESEARCH & SCIENCES

JENRS

www.jenrs.com
ISSN: 2831-4085

Volume 1 Issue 8
August 2022

# EDITORIAL BOARD

## Editor-in-Chief



## Editorial Board Members

# Editorial

In the rapidly evolving landscape of modern science and engineering, four groundbreaking studies offer insights into diverse yet interconnected fields. From biomedical engineering to statistical estimation in sales, magneto-optical qubits, and sustainable requirements engineering, these research papers highlight the strides made in their respective domains.

The first study delves into biomedical engineering, a field that has revolutionized solutions for complex biological problems through the application of engineering principles. This research focuses on hip joint replacements, particularly the comparative analysis of hip replacement implants made from stainless steel (SS) and titanium alloy (Ti6Al4V). Utilizing advanced 3-dimensional finite element analysis with ANSYS2020 and Fusion 360 for modelling, the study evaluates the von-Mises stress, stress locations, and deformation under directional loads. By comparing static structural analysis with different materials and neck angles, this paper provides invaluable insights into the performance of hip prosthesis implants, offering a foundation for future research and improvements in implant design [1].

The second paper addresses the critical aspect of product life cycles, emphasizing the importance of accurate sales data estimation. Using Walmart sales data from 45 stores over 2010-2012, the study explores the integration of additional information—both unbiased and possibly biased—into statistical estimations to enhance accuracy. By minimizing mean squared error and variance, the research illustrates how incorporating external data can refine estimates of weekly sales and account for phenomena such as the holiday effect. This approach not only advances statistical methodologies but also provides practical applications for businesses aiming to optimize their sales strategies [2].

In the realm of quantum computing and information processing, the third paper investigates the properties of magneto-optical qubits through the Faraday rotation effect. The study proposes innovative waveguide geometries for developing various information processing and transmission devices, including logic gates with new architectures. By modeling magneto-optical logic elements capable of performing parallel AND, XOR, and other operations, this research paves the way for a new generation of quantum devices. The potential applications of such devices span multiple fields, from scientific research to industrial processes, underscoring the transformative impact of magneto-optical technologies [3].

Finally, the fourth paper explores the evolving field of Requirements Engineering (RE) with a focus on sustainability. The proposed approach, CRESustain, integrates sustainability dimensions into the RE process by employing creativity techniques inspired by the Sustainable Development Goals, creative problem-solving methods, and the Karlskrona Manifesto. Using Design Science Research methodology, the study demonstrates how CRESustain can foster discussions on sustainability across technical, economic, social, human, and environmental dimensions. This approach not only enriches the RE process but also aligns software development with broader sustainability goals, addressing the pressing need for sustainable practices in the tech industry.

Together, these studies showcase the innovative spirit and interdisciplinary nature of contemporary research. They not only advance their respective fields but also contribute to a deeper understanding of how technology and creativity can address complex challenges in medicine, business, quantum computing, and software engineering [4].

**References:**


[1] C.M. Wani, S.R. Deshmukh, R.R. Ghorpade, “Studies on Stress Analysis of Hip Prosthesis Implant,” *Journal of Engineering Research and Sciences*, vol. 1, no. 8, pp. 1–11, 2022, doi:10.55708/js0108001.

[2] S. Tarima, Z. Zenkova, “Use of Uncertain External Information in Statistical Estimation,” *Journal of Engineering Research and Sciences*, vol. 1, no. 8, pp. 12–18, 2022, doi:10.55708/js0108002.

[3] S. Egamov, A. Khidirov, M.K.B. ugli, “Magneto-Optical Waveguide Logic Gates and their Applications,” *Journal of Engineering Research and Sciences*, vol. 1, no. 8, pp. 19–26, 2022, doi:10.55708/js0108003.

[4] C. Silveira, V. Santos, L. Reis, H. Mamede, “CRESustain: Approach to Include Sustainability and Creativity in Requirements Engineering,” *Journal of Engineering Research and Sciences*, vol. 1, no. 8, pp. 27–34, 2022, doi:10.55708/js0108004.

**Editor-in-chief**

**Prof. Paul Andrew**

JOURNAL OF ENGINEERING RESEARCH AND SCIENCES

Volume 1 Issue 8 August 2022

# CONTENTS

JENRS

Received: 28 February 2022, Revised: 27 April 2022, Accepted: 20 July 2022, Online: 19 August 2022

DOI: https://dx.doi.org/10.55708/js0108001

# Studies on Stress Analysis of Hip Prosthesis Implant

**Chetan Mohanlal Wani *, Sachin Ratnakar Deshmukh, Ratnakar Raghunath Ghorpade**

School of Mechanical Engineering, Dr. Vishwanath Karad MIT-World Peace University, Pune-411038, Maharashtra India

*Corresponding author: Chetan Wani, , Dr. Vishwanath Karad MIT-World Peace University, Pune-411038, Maharashtra India, +91-7972949080, Chetan.wani101@gmail.com

**ABSTRACT:** Biomedical engineering has become a solution for many biological problems by the application of principles and problem-solving techniques. Pacemakers, artificial bone replacements, 3-D printed organs, and dental replacements are very common examples of an application of engineering in the biomedical field. In medical applications when there is a need for bone replacement in a patient who is suffering from arthritis, the hip joint replacement cannot be avoided. The use of the artificial hip joint is going more popular and has become a need in the case of arthritis. An artificial hip implant is essential for providing initial stability at the place of failure. The comparative study in this field is limited and needs to be studied thoroughly. This paper focuses on a comparative study of hip replacement implants using SS (stainless steel) and Ti6Al4V (titanium alloy). In this study, 3-dimensional finite element analysis (using ANSYS2020) of hip replacement implant is performed by applying directional loads to detect von-mises stress amount, stress locations, and deformation in the implant. Assembly of the hip replacement implant is modeled (using Fusion 360) and static structural analysis is separately done using two different materials (SS and Ti-6Al-4V) for the femoral stem and using HDPE and HDPE/0.25MWCNT/0.15 for acetabular cup and liners respectively. Boundary conditions and loads applied are unchanged while varying parameters are the neck angle of implant and materials used. A similar static structural analysis for the elevated liner and flat liner at three different shell inclinations is done separately using the model which has shown better results. This study will help the researchers for further study on stress analysis of hip prosthesis implants.

**KEYWORDS:** Hip prosthesis, finite element analysis (FEA), Total hip arthroplasty (THA), Stainless Steel (SS), Ti Alloy (Ti-6Al-4V).

## 1. Introduction

The human body has roughly 270 bones when it is born, but by adulthood, it has been lowered to 206 bones since some of the bones have bonded together [1]. The femur seems to be the longest and also highest load-carrying bone in the human body, joining the pelvic in the proximal and the tibia in the distal. Its length fluctuates from individual accounts for around a quarter of the body's height (45–50 cm in general) [2]. In the human body, the hip joint is considered one of the most critical joints. Knee and total hip surgeries are universally acknowledged as efficient and positive treatments for osteoarthritis of the joint [3]. Total hip arthroplasty (THA) is the medical term intended for hip replacement. Year after year, the total number of hip replacement operations is rising [4]. More effort has been made to satisfy the patient's isolated requirements, for example by increasing the range of types and sizes of hip prostheses, a large proportion of THAs become loose after they have been implanted for decades [5]. This joint can decay due to numerous reasons that include osteoarthritis, atrophic arthritis, and avascular necrosis [6]. Stem or head rupture, wear and eventual metallosis illnesses, destabilization owing to bone breakage, necrosis or stress shielding, and infectious agents that develop a biofilm between of implant and the bone are all reasons for implant failure [7]. Strain and stress shielding, as results from the differing rigidity of implant materials and the neighboring bone, is a major concern with hip resurfacing arthroplasty (HRA) [8]. Aseptic loosening of the acetabulum due to stress shielding and altered load distribution within the adjacent bone structure is a common cause of total hip arthroplasty failure [9]. Studies projected that, worldwide, there are nearly one million surgeries of hip replacement done every year [10]. Implants are generally selected based on the patient's age and bone condition; for older patients,

cemented implants are often favored. 2D radiography or preoperative 3D planning tools ensure that the implant and the femur are geometrically compatible [11]. In various actions, the hip joint can carry an upper body weight of up to four times that of the human body weight.

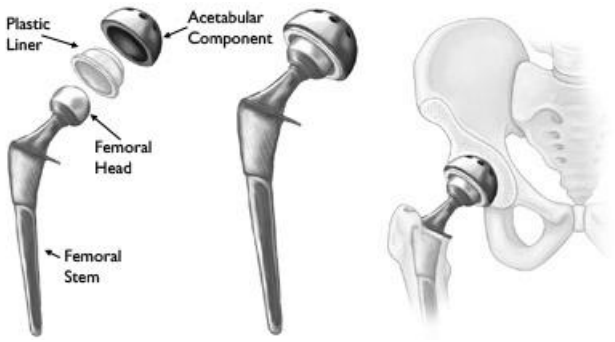


Figure 1: Components in total hip replacement implant

An artificial hip implant is consisting of mainly two components. First is the acetabular element which is placed in the pelvis and the second is a femoral element which includes a femoral stem and ball-like head placing the femoral head. The geometry of the hip replacement implant is shown in figure 1.1. In healthful individuals, the skeletal interaction regions are coated by articular cartilage, a soft and delicate tissue that cushions the endpoints of the pelvis and femur bones and then almost eliminates friction. The Tissue bands hold the ball and joint together [12]. A large proportion of THAs experience loosening after 15-20 years of implantation. Approximately 30% of patients that have undergone total hip replacement need revision of operation [5].

There is proof that adopting bigger femoral head sizes and increased offsets lessen the chance of hip unnecessary displacement by permitting more impingement-free mobility and thereby enhancing the jumping range in both initial and repair unrestricted THA [13].

Yekutiel Katz et al. performed Ex-Vivo tests on four fresh-frozen human femurs and found that the finite element models relying on computed tomography can accurately calculate strains on the femur surfaces and implanted implants at the cement interface [11]. Kaddick et al. investigated static failure loads and peak stresses of physiologically formed carbon fiber reinforced epoxy hip stem using finite-element analysis. At the same forces, they found that flexible implants create larger strains than stiffer implants [14]. Kayabasi and Ekici investigated the impacts of stable, dynamical, and fatigue behavior on three-dimensional shape optimization of titanium and cobalt-chromium alloy hip prostheses using PMMA cemented in the casual walking scenario using the FE approach. They discovered that whereas stem designs are projected to be safe against failure under static stress, collapse can occur during dynamical repetitive loading [15].

Materials used for hip prosthesis implants are studied in detail In this paper. Broadly used materials for the hip joint implant can be distributed into several pairs: polymer to ceramic, metal to metal, metal to polymer, and ceramic to ceramic [16]. The most widely used metals for stem and femoral heads are stainless steel, Ti alloy, and Cr-Co alloy. Polymers are used for the acetabular liner and polymers, composites, or bio metals are used for the acetabular shell. Each material has its advantages and disadvantages. Some of the properties that are considered during the selection of materials are their yield strength, density, young's modulus, hardness, corrosion resistance, biocompatibility, and biodegradability. Further chapters discuss the CAD design, analysis, results, and conclusion for the analysis done on hip prosthesis implant.

## 2. Materials

The materials are selected by considering the human biological environment and by considering the mechanical properties of the human hip bone. The mechanical properties of human bone are shown in table 1.

Table 1: Mechanical properties of human bone

| Density ($Kg/m^3$) | Yield Strength (Pa) | Poisson's Ratio | Young's Modulus (Pa) |
|---|---|---|---|
| 310±60 | 1.14e+8 | 0.62±0.26 | 1.1e+10 - 2e+10 |

There are two primary criteria for selecting materials. Medical requirements are concerned with the material's biocompatibility, while mechanical criteria are concerned with wear resistance, stress concentration, and implant stability [17].

### *2.1. Ti6Al4V*

Ti6Al4V is the most commonly used titanium alloy, making up about half of all titanium options on the market today [18]. Because titanium and titanium alloys are biodegradable, they do not require an intermediary layer of cement-like stainless steel or CrCo alloys. Due to the lower shear resistance, Ti and Ti alloys are wear-resistant [16]. The two Ti-based alloys now accessible for implantation are commercially sterling titanium and Ti–6Al–4V, though Ti-6Al-V4 is taking over commercially sterling titanium because of its superior mechanical strength. Long-term application of Ti alloys causes health issues like Alzheimer's disease and neuropathy, which are mostly driven by aluminum and vanadium excretion [16].

### *2.2. Polymers*

Due to their minimal price and a broad variety of physical and mechanical qualities, polymer materials are utilized in a wide range of uses. Polymers are categorized into two categories depending on how far they last in biological atmospheres:

1. Biodegradable and 2. Biostable Polyethylene (PE), poly (methylmethacrylate) (PMMA), and polyetheretherketone (PEEK) are examples of biostable polymers that are used in hip and dental implants [16]. For hip and knee joints, UHMWPE (ultrahigh molecular weight polyethylene) has been widely employed [16]. Polylactic acid (PLA), polyglycolic acid (PGA), poly lactic-co-glycolic acid (PLGA), and poly e-caprolactone (PCL) are the second family of biodegradable polymers that can break down gradually in the body's physiological milieu into biocompatible compounds [16]. The early study exposed that UHMWPE is an appropriate material for THR.

*2.3. Stainless Steel*

Because of its high Cr content (more than 12 wt %), Materials made of stainless steel are more resistant to a wide range of eroding environments, allowing for the creation of a firmly adhering, corrosion-resistant, and self-curing Cr Cr2O3 coating oxide. The formation of chromium carbides at grain borders does not induce intergranular corrosion in austenitic stainless steel [19]. SS has few applications in medical implants, despite its many benefits as in a presence of chloride, it is susceptible to corroding, leading to the release of harmful metallic ions like chromium and nickel [20]. Implants made of stainless steel have degraded in the body because of pitting, crevice corrosion, corrosion fatigue, fretting corrosion, stress corrosion cracking, and galvanic corrosion, despite these properties [16]. Because chromium in the outermost layer interacts with oxygen, a thin film of adhered and cohesive oxide (passive film) encloses the surface and acts as a rusting barrier [19]. The withstanding ability of austenitic stainless steel with wear is quite low. Sterile slackening of the joint occurs when a large amount of worn fragments is formed. Furthermore, stainless steel has a modulus of roughly 200 GPa, which is significantly more than bone [16] having a modulus in the range of 11-20 GPa. Materials and their properties considered in this study are [21], [22]:

Table 2: Materials and properties used

| Materials | Density ($Kg/m^3$) | Yield Strength (Pa) | Poisson's Ratio | Young's Modulus (Pa) |
|---|---|---|---|---|
| Ti-6Al-4V | 430 | 8.8E+08 | 0.28 | 1.09E+11 |
| HDPE | 964 | 2.97E+07 | 0.42 | 1E+15 |
| HDPE/0.25 MWCNT/0.15 | 964 | 4.2E+07 | 0.43 | 1.5E+09 |
| Stainless Steel | 8000 | 2.15E+08 | 0.27 | 2.1E+11 |

- Acetabular shell: HDPE
- Liner: HDPE/0.25MWCNT/0.15
- Femoral head: Ti6Al4V/Stainless steel
- Femoral stem: Ti6Al4V/Stainless steel

## 3. Methodology

*3.1. Design*

In total hip arthroplasty, a variety of designs are routinely employed. Profile and shape are significant parameters at design time distortion [23]. In this study, the total assembly of an artificial hip implant is divided into four components that are 1] Acetabular shell 2] Acetabular liner (flat/elevated at 10°) 3] Femoral head 4] Femoral stem. The design and assembly are done in the Fusion 360 software. Acetabular shell has an outside diameter of 52 mm and an inside diameter of 38 mm, an outer diameter of both flat and elevated liner is considered as 28 mm and outer diameter as 38 mm, the elevation of the elevated liner is kept as 10° [21]. The diameter of the femoral head is 28 mm, and the length of the femoral stem is taken as 120 mm [22]. Even across smaller group measurements, the angle of the femoral neck concerning the shaft (the neck-shaft angle, NSA) varies greatly between contemporary humans and previous hominins. Adult figures for modern humans are typically within the range of 120 and 140 degrees, while readings as low as 120 degrees and as high as 140 degrees are not unusual (known as coxa varus and coxa valgus, respectively). [24]. As per the studies by Ian Gilligan [24], NSA varies from 115°-140° (range of 25° in 47 Indian samples, σ= 5, mean= 129.9°). So, different assemblies were done by changing the neck angle by 120°, 130°, and 140° [22]. Dimensions for the design are taken from [21]. The assembly file is then exported into .iges format for further analysis.

More detailed dimensions of the CAD model are given in following figure 2 (a-e):

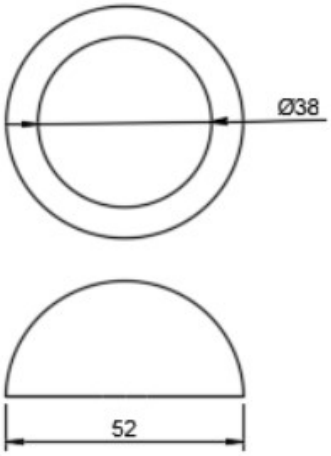


Figure 2 a): Acetabular shell

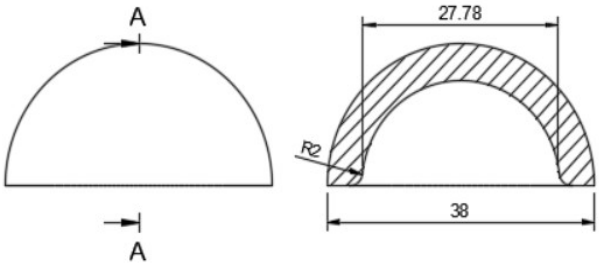


Figure 2 b): Acetabular flat liner

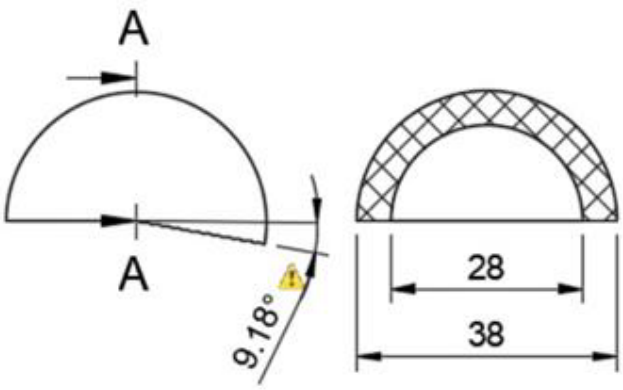


Figure 2 c): Acetabular elevated liner

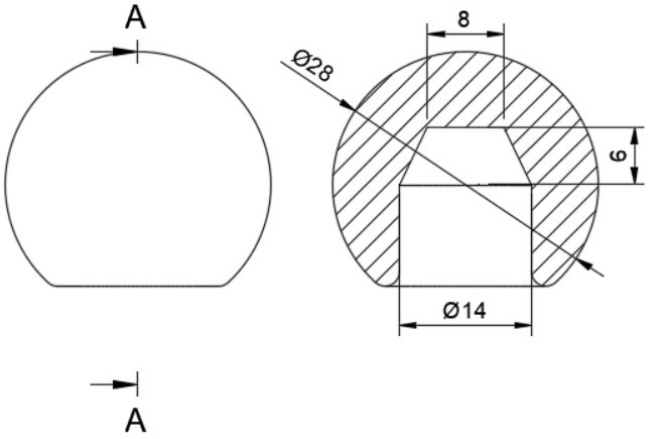


Figure 2 d): Femoral head

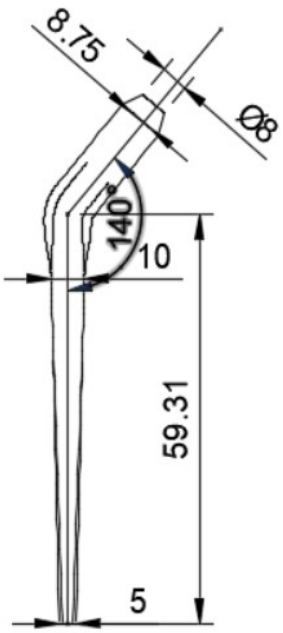


Figure 2 e): Femoral stem (As per the paper number [24], the neck-shaft angle varies between 120°-140°. In the above figure angle of 140° is considered only for visual representation.)

### *3.2. Finite Element Analysis*

The finite element method is a commonly used method of computer technology for dental implant research [25]. Biomechanical characteristics of the implant-bone compound are a strain/stress distribution that may be important in selecting the best implant [11]. Finite element analyses (FEA) may now provide this biomechanical knowledge by identifying the implant that generates the least divergence in the strain distribution relative to the strain distribution before the breakage of a bone [11]. These methods are widely employed in the fields of autos, aeronautics, as well as various structural and fluid dynamic applications to solve multi-physics difficulties [26]. On the spot, a computer simulation was performed. 'ANSYS Workbench 2020' platform is used for finite element analysis in this study. The materials which are to be used in the analysis were added and the properties for each material were provided along with their values. The materials were assigned for each component in the assembly i.e. HDPE for acetabular cup, HDPE/0.25MWCNT/0.15BNNP for acetabular liners (flat and elevated), stainless steel, and Ti6Al4V assigned to femoral stem and head. For every iteration, the material is chanfromd from stainless steel to Ti6Al4V. After assigning materials, 3 contact regions were provided as bonded for cup and liner, frictional between head and liner by providing frictional coefficient as 0, again bonded contact were provided to the stem and head. The next step was dividing the complete assembling into small elements by meshing. A tetrahedron mesh was used as the mesh element with a mesh size of 2 mm. Tetrahedron mesh is used because it discretizes the complex geometries better in equal parts and a size of 2 mm was provided for fine meshing. The boundary conditions [22] were provided to the assembly model. Boundary conditions were kept unchanged for the analysis of each assembly model. Total 4-point loads were applied. One load of 3700 N in the reversed direction was on the top surface of the stem the and other 3 loads were applied on the inner surface of the shell on the X, Y, and Z-axis having values of 1241 N, -4519 N, and 1222 N respectively as shown in following figure 3 (a,b):

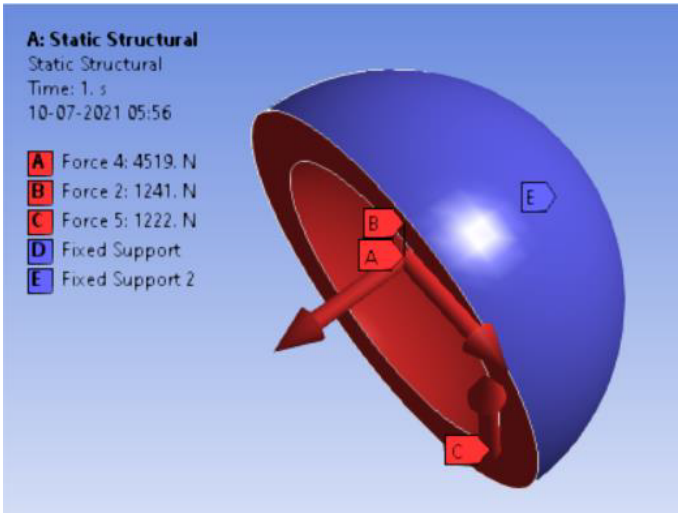


Figure 3 a): Acetabular cup

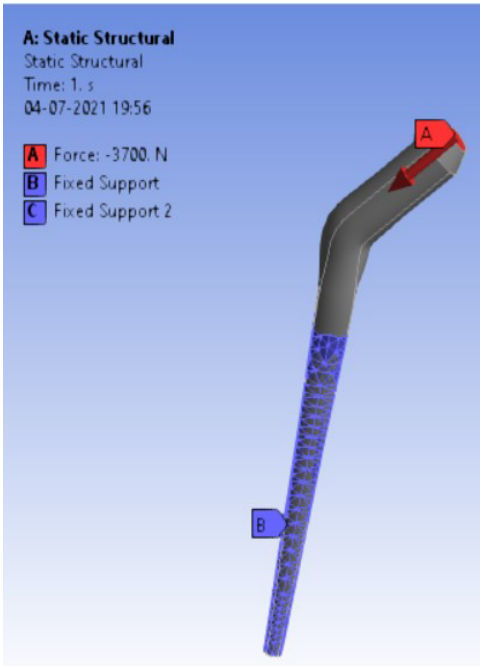


Figure 3 b): Femoral stem

After applying boundary conditions, solutions that are needed to find were added to the list of solutions.

## 4. Results and Discussion

After the analysis in static structural, results were calculated in the form of von-mises stresses induced in MPa and the total deformation generated in mm in each assembly model of hip prosthesis implant. The following figures show the results:

Von-mises stress for different neck angle angles [figure 4 (a-f)]:

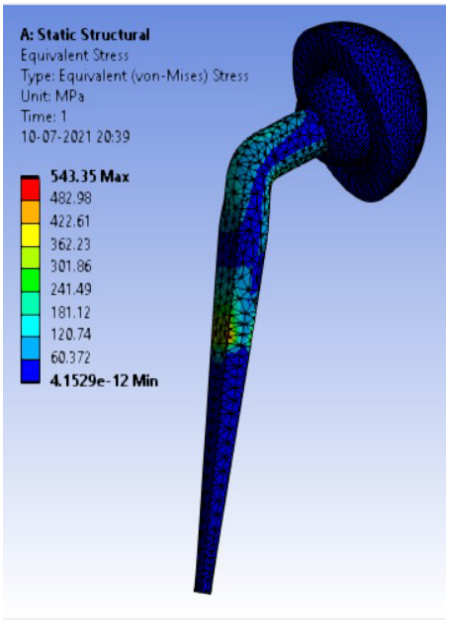


Figure 4 a): 120° (SS)

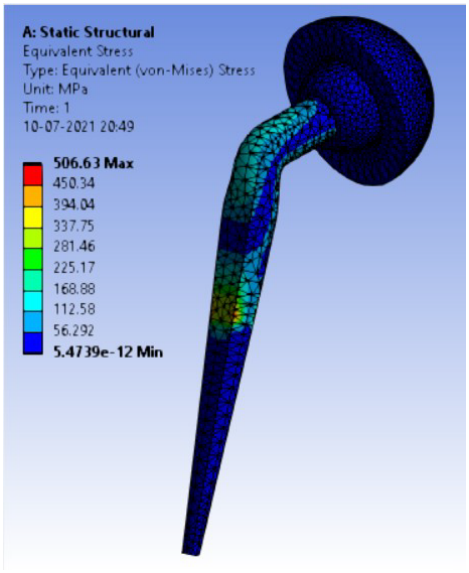


Figure 4 b): 120°(Ti6Al4V)

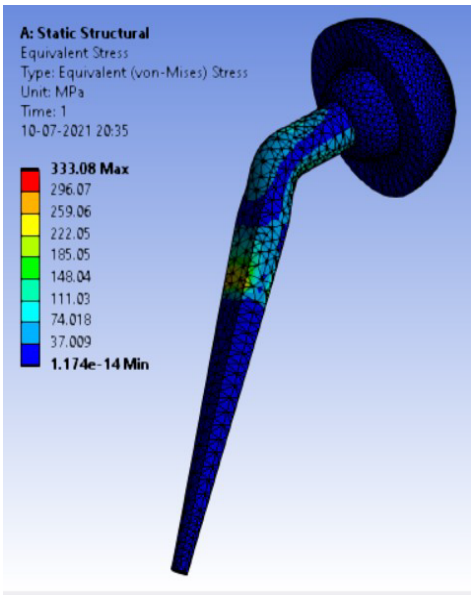


Figure 4 c): 130° (SS)

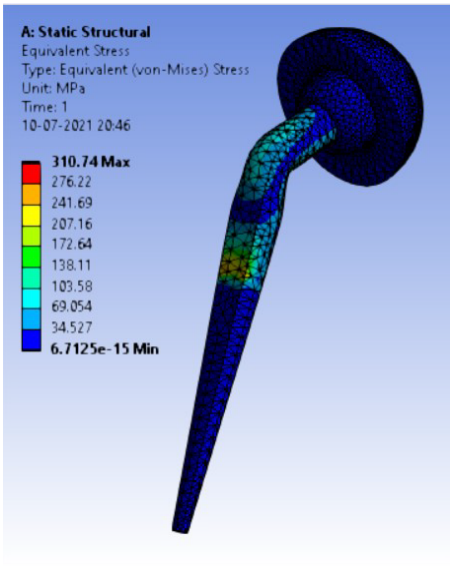


Figure 4 d): 130° (Ti6Al4V)

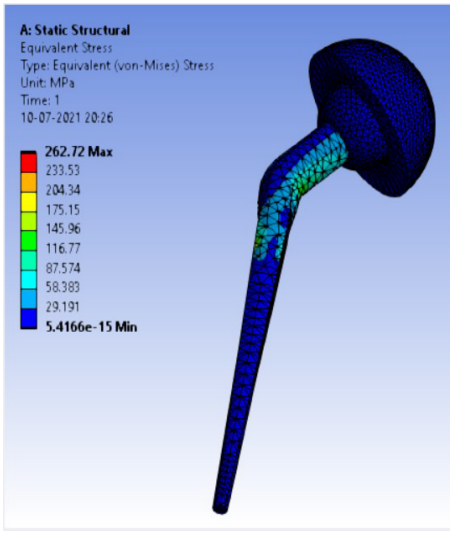


Figure 4 e): 140° (SS)

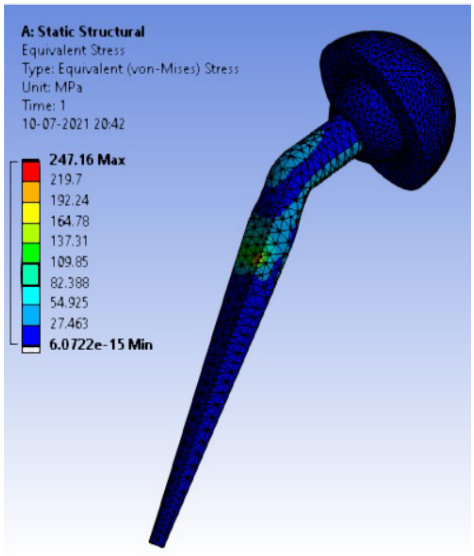


Figure 4 f): 140° (Ti6Al4V)

Displacement for different neck angle-angle [figure 5 (a-f)]:

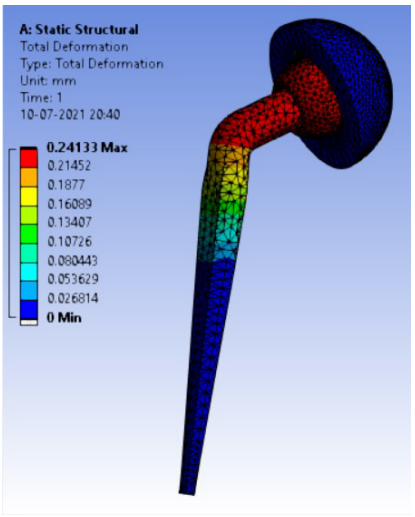


Figure 5 a): 120° (SS)

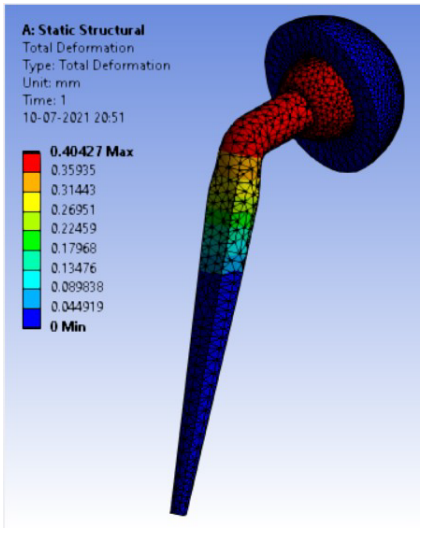


Figure 5 b): 120° (Ti6Al4V)

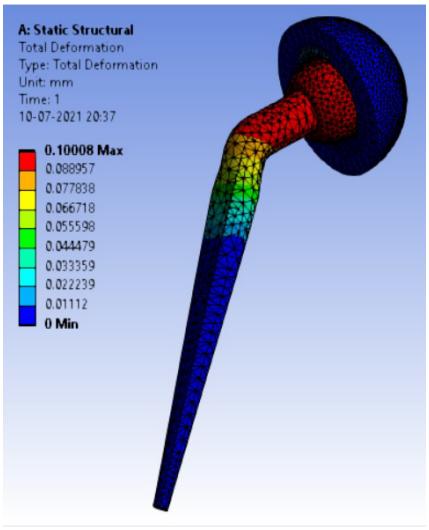


Figure 5 c): 130° (SS)

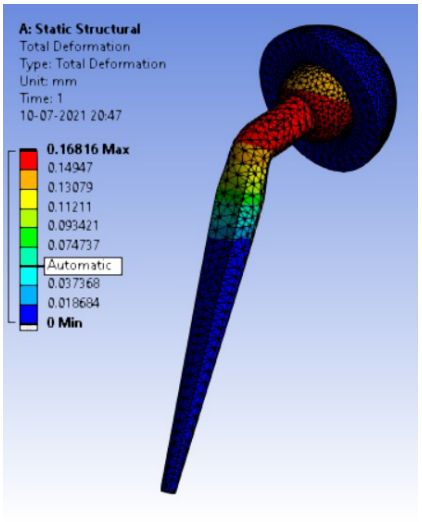


Figure 5 d): 130° (Ti6Al4V)

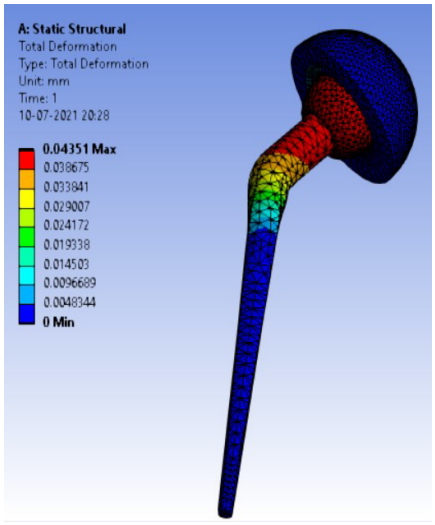


Figure 5 e): 140° (SS)

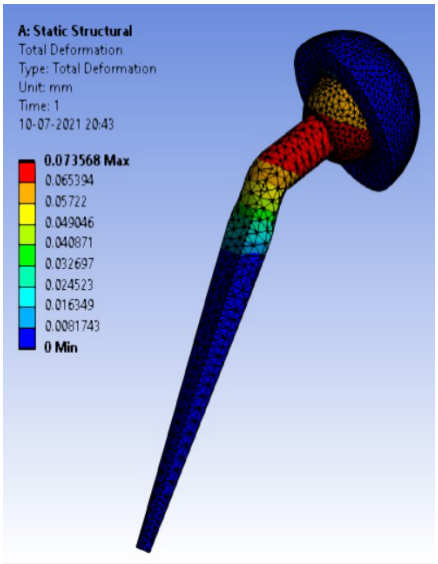


Figure 5 f): 140° (Ti6Al4V)

Von-mises stress for the different inclination of the shell using flat and elevated liner [figure 6 (a-f)]:

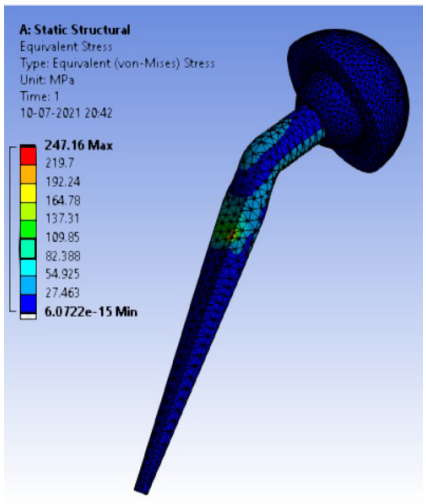


Figure 6 a): 90° (Flat)

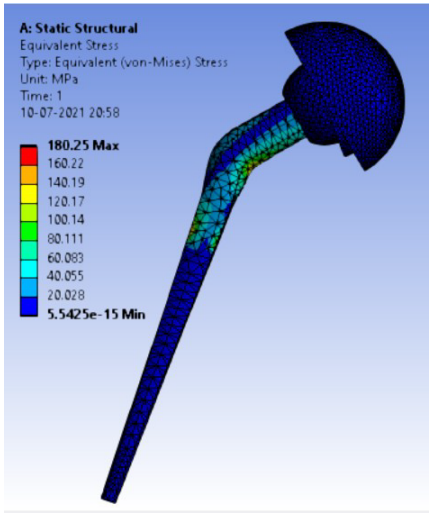


Figure 6 b): 90° (ELevated)

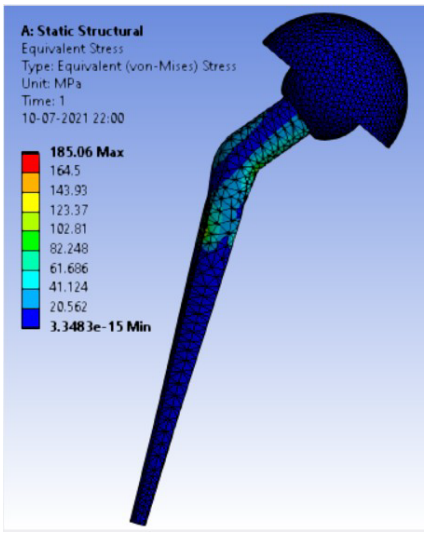


Figure 6 c): 75° (Flat)

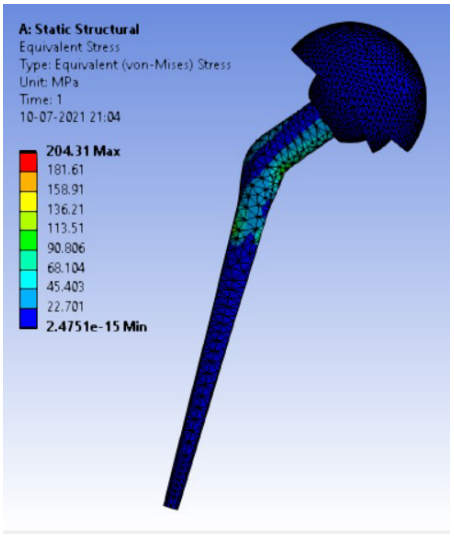


Figure 6 d): 75° (Elevated)

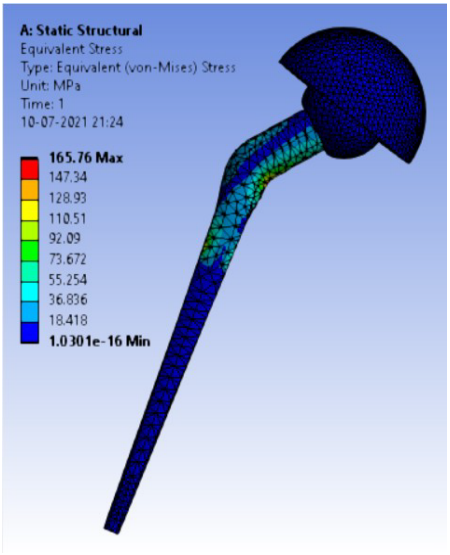


Figure 6 e): 65° (Flat)

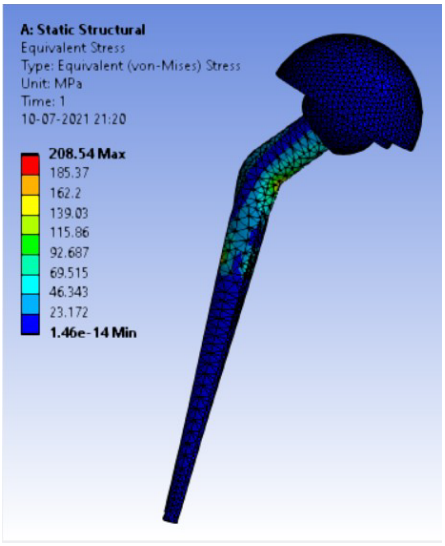


Figure 6 f): 65° (Elevated)

Displacement for the different inclination of the shell using flat and elevated liner [figure 7 (a-f)]:

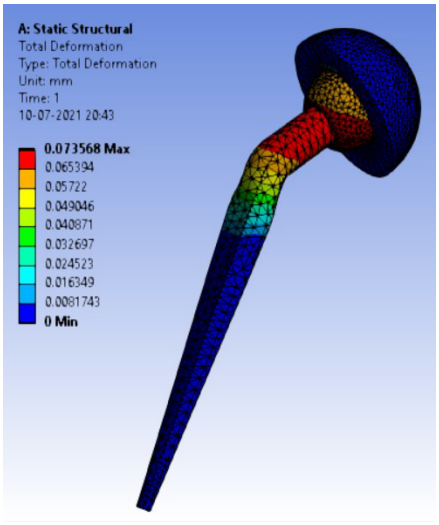


Figure 7 a): 90° (Flat)

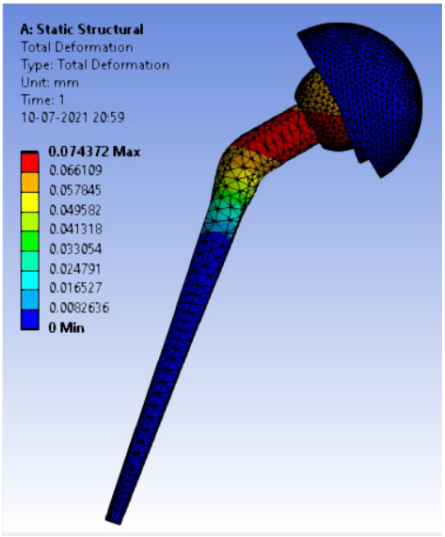


Figure 7 b): 90° (Elevated)

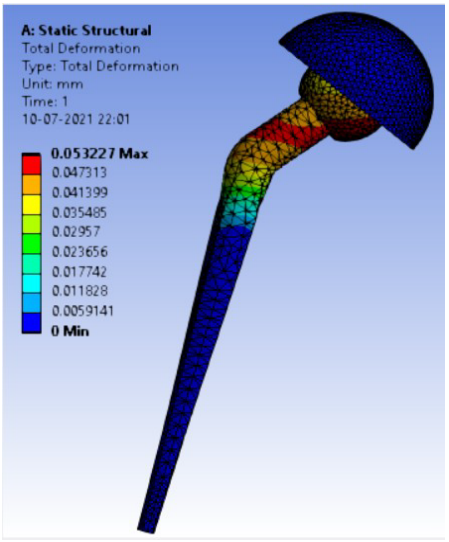


Figure 7 c): 75° (Flat)

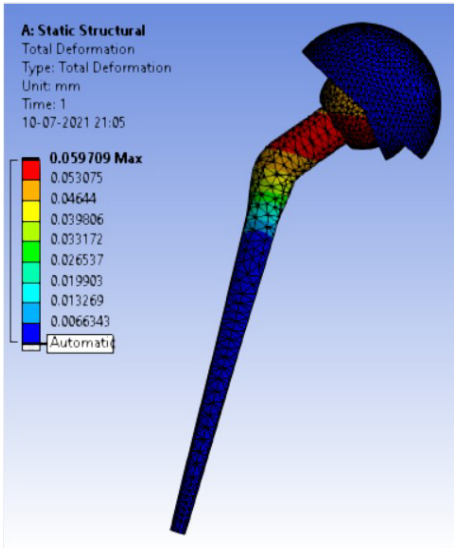


Figure 7 d): 75° (Elevated)

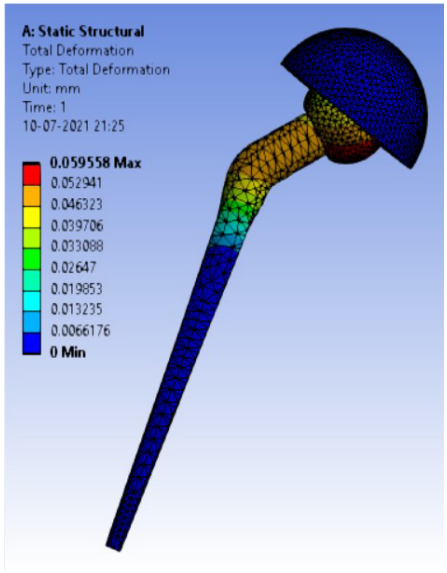


Figure 7 e): 65° (Flat)

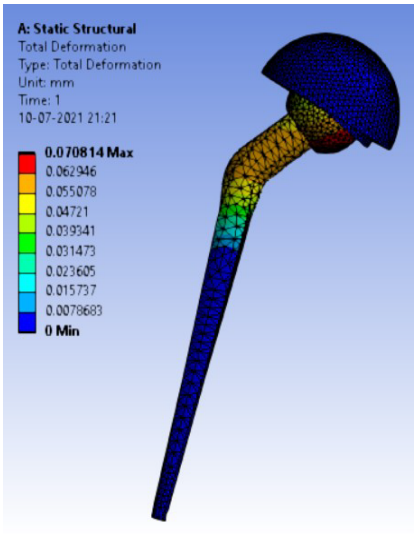


Figure 7 f): 65° (Elevated)

Table 3: Result table for different neck angle angle

| Sr. No. | Variable Parameter (Stem angle 'ø') | Equivalent Stress (MPa) | | Displacement (mm) | |
|---|---|---|---|---|---|
| | | Ti Alloy | Stainless Steel | Ti Alloy | Stainless Steel |
| 1. | 120° | 506.63 | 543.35 | 0.40427 | 0.24133 |
| 2. | 130° | 310.74 | 333.08 | 0.16816 | 0.10008 |
| 3. | 140° | 247.16 | 262.72 | 0.07357 | 0.04351 |

Table 4: Result table for different shell inclination

| Sr. No. | NSA (neck-shaft angle) | Equivalent stress (MPa) | | |
|---|---|---|---|---|
| | | Stress in stem from the studies done by Dannana Dimple et.al. [22] | Ti Alloy | Stainless Steel |
| 1. | 100° | 336 | - | - |
| 2. | 110° | 238.56 | - | - |
| 3. | 120° | 208.32 | 506.63 | 543.35 |
| 4. | 130° | 204.96 | 310.74 | 333.08 |
| 5. | 140° | 147.84 | 247.16 | 262.72 |

The results for all the equivalent stresses and displacements are given in table 3 & table 4. Figure 8 shows the graph of the influence of stem angle on the behavior of equivalent stress for SS and Ti6Al4V. Likewise, Figure 9 describes the graph for the influence of shell inclination on the behavior of equivalent stress.

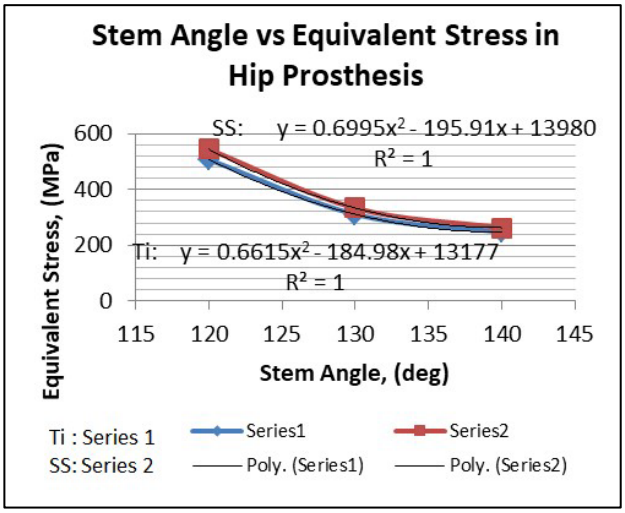


Figure 8: Behaviour of equivalent stress with change in stem angle (neck angle-angle)

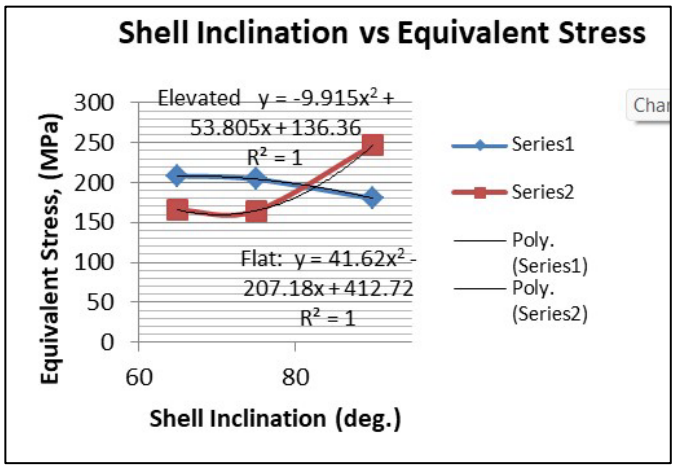


Figure 9: Behaviour of equivalent stress with the change in shell inclination

As the neck angle (ø) increases, the amount of equivalent stress is decreased. The maximum value of stress is at an angle of 120° in stainless steel i.e. 543.35 MPa and the minimum value of stress is at 140° in Ti alloy i.e. 247.16 MPa. The weight of stainless steel is more than that of Ti-6Al-4V. Also, in all the cases, more stress is observed in SS than stress observed in Ti-6Al-4V. As the inclination of the acetabular shell increases, assemblies that used elevated liners have increasing values of von-mises stress than the assemblies that used flatliners. From the results in this study, if we consider other properties of liners like the ability to provide support and motion stability, elevated liners used in assembly at an angle of 75° showed better results.

Table 5: Comparison of the results

| Sr. No. | Variable Parameter (Inclination of shell) | Equivalent Stress (MPa) | | Displacement (mm) | |
|---|---|---|---|---|---|
| | | Elevated | Flat | Elevated | Flat |

| | | | | | |
|---|---|---|---|---|---|
| 1. | 90° | 180.25 | 247.16 | 0.074372 | 0.07357 |
| 2. | 75° | 204.31 | 164.84 | 0.05971 | 0.05899 |
| 3. | 65° | 208.54 | 165.76 | 0.0708 | 0.05956 |

A comparison of the results from the studies done by Dannana Dimple et. al. and the results from this study are given in table 5. From both the studies it can be observed that, as the NSA is increased, the stresses generated showed decreasing values. It is observed in both the studies that stress amount at an NSA of 140° is the least. Study by Dannana Dimple et. al. is based on the FEA of stem separately unlike in the presented study, the FEA is done on whole assembly of hip implant.

## 5. Conclusion

If the ratio of displacement concerning stress is considered, stainless steel has shown better results than that of Ti6Al4V. That is, if the same amount of stress is considered in both materials, the displacement in stainless steel will have a lower amount than Ti6Al4V. Also, unlike stainless steel, Ti6Al4V is biodegradable and the stress generated in Ti6Al4V is less for the same boundary conditions, Ti6Al4V would be preferable over stainless steel. Ti6Al4V implant at an angle of 140° is preferable for surgeries where a 140° neck angle-angle is allowed. As the inclination of the acetabular shell increases, assemblies that used elevated liners have increasing values of von-mises stress than the assemblies that used flatliners. There is very little difference between the displacements of elevated and flatliners at each angle. As the surface contact area in elevated liners is larger than in flatliners, elevated liners provide support and more stability to the movement of the femoral head whereas flat liners provide less stress-affected area. Surgeons should take these properties under consideration before using the liners. From the results in this study, if we consider other properties of liners like the ability to provide support and motion stability, elevated liners used in assembly at an angle of 75° showed better results so, it is preferable for use in hip implants.

## Conflict of Interest

The authors declare no conflict of interest.

## References

[1]. C. K. N., S. B. N., Z. M., and S. S. B., "Finite Element Analysis of Different Hip Implant Designs along with Femur under Static Loading Conditions," *Biomed Phys Eng.*, pp. 507-516, 2019, doi: 10.31661/jbpe.v0i0.1210.

[2]. Y. E. Delikanli and M. C. Kayacan, "Design, manufacture, and fatigue analysis of lightweight hip implants," *Journal of Applied Biomaterials and Fundamental Materials*, pp. 1-19, May 2019, doi: 10.1177/2280800019836830.

[3]. S. Kurtz, F. Mowat, K. Ong, N. Chan, E. Lau, and M. Halpern, "Prevalence of primary and revision total hip and knee arthroplasty in the United States from 1990 through 2002," *J. Bone Jt Surg. Am.*, vol. 87, no. 7, pp. 1487-1497, 2005.

[4]. S. Kurtz, K. Ong, E. Lau, F. Mowat, and M. Halpern, "Projections of primary and revision hip and knee arthroplasty in the United States from 2005 to 2030," *J. Bone Jt Surg. Am.*, vol. 89, no. 4, pp. 780-785, 2007, doi: 10.2106/JBJS.F.00222.

[5]. X. Li, D. Li, Q. Lian, H. Guo, and Z. Jin, "The effect of stem structure on stress distribution of a custom-made hip prosthesis," *Proceedings of the Institution of Mechanical Engineers, Part H: Journal of Engineering in Medicine*, pp. 1-12, Nov. 2010, doi: 10.1243/09544119JEIM768.

[6]. R. B. Taqriban, R. Ismail, J. Jamari, and A. P. Bayuseno, "Finite element analysis of artificial hip joint implant made from stainless steel 316L," *Bali Medical Journal*, vol. 10, no. 1, pp. 448-452, 2021, doi: 10.15562/bmj.v10i1.2236.

[7]. A. Fiorentino, G. Zarattini, U. Pazzaglia, and E. Ceretti, "Hip prosthesis design. Market analysis, new perspectives and an innovative solution," *Procedia CIRP*, vol. 5, pp. 310-314, 2013, doi: 10.1016/j.procir.2013.01.061.

[8]. D. Vogel, M. Wehmeyer, M. Kebbach, H. Heyer, and R. Bader, "Stress and strain distribution in femoral heads for hip resurfacing arthroplasty with different materials: A finite element analysis," *Journal of the Mechanical Behavior of Biomedical Materials*, vol. 104115, pp. 1-11, 2021, doi: 10.1016/j.jmbbm.2020.104115.

[9]. D. Vogel, M. Klimek, M. Saemann, and R. Bader, "Influence of the Acetabular Cup Material on the Shell Deformation and Strain Distribution in the Adjacent Bone—A Finite Element Analysis," *Materials*, vol. 13, no. 6, pp. 1-16, 2020, doi: 10.3390/ma13061372.

[10]. J. M. Wilkinson, N. F. A. Peel, R. A. Elson, I. Stockley, and R. Eastell, "Measuring the bone mineral density of the pelvis and proximal femur after total hip arthroplasty," *J. Bone Jt Surg. Br.*, vol. 83, no. 2, pp. 283-288, 2001.

[11]. Y. Katz, O. Lubovsky, and Z. Yosibash, "Patient-specific finite element analysis of femurs with cemented hip implants," *Clinical Biomechanics*, vol. 57, pp. 1-32, June 2018, doi: 10.1016/j.clinbiomech.2018.06.012.

[12]. H. M. Kamel, "Modeling And Simulation Of A Hip Prosthesis Implantation," *Proceedings of the 27th Int. AMME Conference*, pp. 1-13, Apr. 2018, doi: 10.21608/AMME.2018.35024.

[13]. Y. Warschawski, S. P. Garceau, D. A. Joly, P. Kuzyk, A. Gross, and O. Safir, "The Effect of Femoral Head Size, Neck Length, and Offset on Dislocation Rates of Constrained Acetabular Liners," *The Journal of Arthroplasty*, vol. 35, no. 7, pp. 1-19, 2020, doi:10.1016/j.arth.2020.07.067.

[14]. C. Kaddick, S. Stur, and E. Hipp, "Mechanical simulation of composite hip stems," *Medical Engineering & Physics*, vol. 19, no. 5, pp. 431-439, 1997, doi: https://doi.org/10.1016/S1350-4533(97)00008-8.

[15]. O. Kayabasi and B. Ekici, "The effects of static, dynamic and fatigue behavior on three-dimensional shape optimization of the hip prosthesis by finite element method," *Materials & Design*, vol. 28, no. 8, pp. 2269-2277, 2007, doi: 10.1016/j.matdes.2006.08.012.

[16]. S. Ghalme and Y. J. Bhalerao, "Biomaterials in Hip Joint Replacement," *International Journal of Materials Science and Engineering*, vol. 4, no. 2, pp. 1-14, June 2016, doi: 10.17706/ijmse.2016.4.2.113-125.

[17]. A. K. Bhawe, K. M. Shah, S. Somani, S. S. B, S. B. N, M. Zuber, and C. K. N., "Static structural analysis of the effect of change in femoral head sizes used in Total Hip Arthroplasty using finite element method," *Cogent Engineering*, vol. 9, no. 1, pp. 1-14, Jan. 2022, doi: 10.1080/23311916.2022.2027080.

[18]. S. Liu and Y. C. Shin, "Additive manufacturing of Ti6Al4V alloy: A review," *Materials and Design*, vol. 164, pp. 1-23, 2019, doi: 10.1016/j.matdes.2018.107552.

[19]. M. K. Abbass, S. A. Ajeel, and H. M. Wadullah, "Biocompatibility, Bioactivity and Corrosion Resistance of Stainless Steel 316L Nano

coated with $TiO_2$ and $Al_2O_3$ by Atomic Layer Deposition Method," *Journal of Physics: Conference Series*, vol. 1032, no. 1, pp. 1-16, 2018, doi: 10.1088/1742-6596/1032/1/012017.

[20]. A. Bekmurzayeva, W. J. Duncanson, H. S. Azevedo, and D. A. Kanayeva, "Surface modification of stainless steel for biomedical applications: Revisiting a century-old material," *Materials Science and Engineering: C*, vol. 93, pp. 1073-1089, Aug. 2018, doi: 10.1016/j.msec.2018.08.049.

[21]. N. Kaku, A. Tanaka, H. Tagomori, and H. Tsumura, "Finite Element Analysis of Stress Distribution in Flat and Elevated-Rim Polyethylene Acetabular Liners," *Clinics in Orthopaedic Surgery*, vol. 12, no. 3, pp. 291-297, 2020, doi: 10.4055/cios19145.

[22]. D. Dimpal, M. Shruti, and S. K. Sahu, "Finite Element Analysis of HDPE-Based Hybrid Nanocomposite for Potential Use As Liner Material for Hip Prosthesis," *Journal of Advances in Engineering Design*, pp. 305-313, 2021, doi: 10.1007/978-981-33-4684-0_31.

[23]. C. K. N., M. Zuber, S. B. N., S. S. B, and C. R. Kini, "Static structural analysis of different stem designs used in total hip arthroplasty using finite element method," *Heliyon*, vol. 5, e01767, pp. 1-8, 2019, doi: 10.1016/j.heliyon.2019.e01767.

[24]. I. Gilligan, S. Chandraphak, and P. Mahakkanukrauh, "Femoral neck-shaft angle in humans: variation relating to climate, clothing, lifestyle, sex, age and side," *Journal of Anatomy*, vol. 223, no. 2, pp. 133-151, 2013, doi: 10.1111/joa.12073.

[25]. R. R. Ghorpade and S. Yelekar, "Computational and Experimental Studies in Threaded Dental Implant Research: A review," *e-Journal of Dentistry*, vol. 3, no. 4, pp. 1-10, Oct.-Dec. 2013.

[26]. C. K. N., S. B. N., M. Zuber, and S. S. B, "Evolution of different designs and wear studies in total hip prosthesis using finite element analysis: A review," *Cogent Engineering*, vol. 9, no. 1, pp. 1-31, 2022, doi: 10.1080/23311916.2022.2027081.



**CHETAN MOHANLAL WANI** has done his bachelor's degree from K. J. College of Engineering and Management Research institution in 2019. He is pursuing his master's degree from MIT- World Peace University.

His research work includes hip prosthesis implants.

**SACHIN RATNAKAR DESHMUKH** has done his bachelor's degree from Shivaji University in 2003. He has completed his master's degree from Savitribai Phule University, Pune in 2010. He is pursuing his PhD degree in Mechanical Engineering from MIT- World Peace University.

His research work includes biomaterial additive manufacturing.

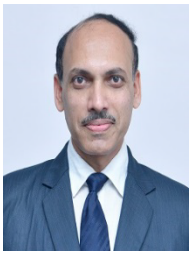

**RATNAKAR RAGHUNATH GHORPADE** has done his bachelor's degree from Shivaji University in 2003. He has completed his master's degree from Pune University in 2010. He has completed his PhD degree in Mechanical Engineering from Savitribai Phule University, Pune in 2017. He has 22 years of experience in teaching, research and industry. Total 50+ publications are at his credit in national/international journals and conferences. He has authored book in his field of interest as Tribology, Robotics, and Strength of Machine Elements. He has worked extensively to simplify root canal obturation procedure, and currently working on his research area in the team of doctors.

Received: 20 January 2022, Revised: 03 March 2022, Accepted: 26 July 2022, Online: 19 August 2022
DOI: https://dx.doi.org/10.55708/js0108002

# Use of Uncertain External Information in Statistical Estimation

**Sergey Tarima** *,[1], **Zhanna Zenkova** [2]

[1] Medical College of Wisconsin, Division of Biostatistics, Institute for Health and Equity, Wauwatosa, Wisconsin, 53226, USA
[2] National Research Tomsk State University, Institute of Applied Mathematics and Computer Science, Tomsk, 634002, Russia
*Corresponding author: Sergey Tarima, 8701 Watertown Plank Rd., Wauwatosa, WI, 53225, USA & starima@mcw.edu

**ABSTRACT:** A product's life cycle hinges on its sales. Product sales are determined by a combination of market demand, industrial production, logistics, supply chains, labor hours, and countless other factors. Business-specific questions about sales are often formalized into questions relating to specific quantities in sales data. Statistical estimation of these quantities of interest is crucial but restricted availability of empirical data reduces the accuracy of such estimation. For example, under certain *regularity conditions* the variance of maximum likelihood estimators cannot be asymptotically lower than the Cramer-Rao lower bound. The presence of additional information from external sources therefore allows the improvement of statistical estimation. Two types of additional information are considered in this work: unbiased and possibly biased. In order to incorporate these two types of additional information in statistical estimation, this manuscript minimizes mean squared error and variance. Publicly available Walmart sales data from 45 stores across 2010-2012 is used to illustrate how these statistical methods can be applied to use additional information for estimating weekly sales. The *holiday effect* (sales spikes during holiday weeks) adjusted for overtime trends is estimated with the use of relevant external information.

**KEYWORDS** Additional information, Minimum variance, Minimum mean squared error, Statistical estimation

## 1. Introduction

Sales data is highly important in a product's life cycle. Sales data is the place where the market demand and industrial supply meet and balance each other to impact inventory management, logistics, supply chains, and more. There are many business-specific questions sales data help address. Typically, these questions are formalized into quantities determined by sales data. Business owners may be interested in the impact of an advertisement campaign, the effect of a holiday on sales, or seasonal trends. Since sales data widely fluctuate, these quantities are considered to be random variables.

The behaviours of these random quantities (i.e. random variables) are described by their probability distributions, estimated with previously collected observations. In [1], the author uses sales data and considers exponential and normal models to reduce the Total Operating Cost. In [2], the authors combine online reviews and historic sales data to forecast sales. In [3], the authors suggest to maximize the direct profit based on both maximization of profit and parameter estimation.

Many of these statistical methods rely on regular estimators– the estimators which have two finite moments. This means that the central limit theorem is applicable, and external information (e.g., averaged sales) known with some uncertainty (e.g., variance) can be incorporated in the statistical estimation procedure to improve accuracy. In [4], Tarima and Pavlov propose a method for incorporating uncertain external information in statistical estimation. [4] and [5] postulate the unbiasedness of additional information. This, for example, means that in different stores the expected sales are the same. [6] derived asymptotic relative efficiency of the estimators proposed in [4]. Previously published data were used in statistical estimation in [7].

It is possible that the external information may estimate a different quantity, leading to a biased external estimate of a quantity of interest. To account for such bias, mean squared error (MSE) is minimized instead in [8, 9]. External information given in the form of a set of possible values is used in [10]–[11], MSE is also minimized. In [12], the author used additional quantile information.

This manuscript shows how external information on sales can be used under (1) the assumption that the external information came from an unbiased data source and (2) that the external data source can be very different to assume unbiasedness. This manuscript is an updated and extended version of a proceedings paper [13] where similar statistical methodology was applied to newsvendor-type problems. Section 3 presents main mathematical results for combining empirical and external data summarized by sample means and their variances. Sections 2 and 4 use these statistical methods for estimating the adjusted holiday effect using publicly available weekly sales data for Walmart stores in

2010-2012. The example was implemented in R [14], see Appendix for the relevant R code.

Table 1: Parameters and their estimators; $E$ denotes mathematical expectation.

| Quantity | Description | Example |
|---|---|---|
| $\theta$ | a parameter of interest | an adjusted effect |
| $\eta$ | an auxiliary parameter | an unadjusted effect |
| $\widehat{\theta}$ | an estimator of the parameter of interest based on the current data | an estimator of the adjusted effect based on the current dataset |
| $\widehat{\eta}$ | an estimator of the auxiliary parameter based on the current dataset | an estimator of the unadjusted effect based on the current dataset |
| $\widetilde{\eta}$ | an estimator of the auxiliary parameter based on an external dataset | an estimator of the unadjusted effect based on the external dataset |
| $\delta$ | bias ($\delta$=$E\widehat{\eta} - E\widetilde{\eta}$) | difference between the adjusted and unadjusted effects |
| $\widehat{\delta}$ | estimated bias ($\widehat{\delta}$=$\widehat{\eta} - \widetilde{\eta}$) | estimated difference between the adjusted and unadjusted effects |

Table 2: Table of regression coefficients for modelling log (weekly sales) ["store id" = 1]; $w$ is a week, $h$ is a holiday indicator, $pS$ is a previous weekly sales, and $p2S$ is the sales from two weeks ago.

| Variable | Estimate | Std. Error | t-value | P-value |
|---|---|---|---|---|
| $(Intercept)$ | -152.2171 | 105.9820 | -1.4363 | 0.1533 |
| $w$ | 0.0289 | 0.0053 | 5.4609 | < 0.0001 |
| $w^2$ | -0.0014 | 0.0002 | -6.1215 | < 0.0001 |
| $w^3$ | 0.0000 | 0.0000 | 6.5850 | < 0.0001 |
| $h$ | **0.0896** | 0.0277 | 3.2409 | 0.0015 |
| $\log(pS)$ | 61.3359 | 11.8651 | 5.1694 | < 0.0001 |
| $\log\left(pS^2\right)$ | -2.1452 | 0.4146 | -5.1743 | < 0.0001 |
| $\log(p2S)$ | -48.3027 | 11.8440 | -4.0782 | 0.0001 |
| $\log\left(p2S^2\right)$ | 1.6799 | 0.4134 | 4.0636 | 0.0001 |
| $year$ | 0.0373 | 0.0087 | 4.2716 | < 0.0001 |

## 2. Illustrative Example

Walmart weekly sales data for a sample of 45 Walmart stores over the period of 2010-2012 became available to public via a Kaggle competition (www.kaggle.com). This dataset was later used by researchers and data scientists for research and educational purposes, see [15]–[16].

For illustrative purposes, the dataset is reduced down to four variables:

- "Store ID": 1 though 45,
- "Date": a week of sales (48 weeks in 2010, 52 weeks in 2011 and 43 weeks in 2012)
- "Sales": total weekly sales, and
- "Holiday": a holiday indicator.

To illustrate the overtime pattern associated with sales within this dataset, a linear autoregressive model was fitted to model weekly sales on a logarithmic scale using the first store data ("store id" = 1). The model's table of regression coefficients is shown in Table 2.

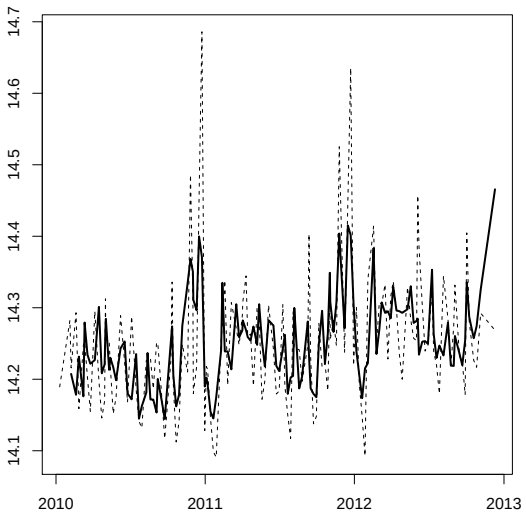


Figure 1: Log(Weekly sales) (dashed line) and their predicted values using the regression model shown in Table 2 ("store id = 1").

Consider the objective of estimating a holiday effect controlling for the overtime sales pattern. The overtime sales pattern controls for the yearly linear effect, the cubic approximation yearly seasonality, and the quadratic approximation of sales within the two previous weeks. The holiday effect adjusted for this overtime pattern is estimated by the regression coefficient and is equal to 0.0896 for store #1. Since the modelling is completed on the logarithmic scale, the effect on total sales is multiplicative and is equal to 1.0937 (= exp (0.0896)), meaning that controlling for the overtime trend ≈ 9.4% increase in total sales is anticipated. This is the adjusted effect, which is different from the unadjusted holiday effect. The unadjusted effect, in our definition, is a proportional increase during holiday weeks as compared to non-holiday weeks. This effect can be estimated by a simple linear regression model reported in Table 3: the unadjusted effect is expressed by the regression coefficient 0.0711, leading to an unadjusted increase in sales ≈ 7.4% (exp (0.0711) =1.0737).

Table 3: Table of regression coefficients for modelling log(weekly sales) ["store id" = 1]; simple linear regression, unadjusted analysis.

| Variable | Estimate | Std. Error | t-value | P-value |
|---|---|---|---|---|
| $(Intercept)$ | 14.2477 | 0.0079 | 1802.197 | < 0.0001 |
| $Holiday$ | **0.0711** | 0.0299 | 2.378 | 0.0187 |

Let's assume that a researcher is able to get access to

nine stores and perform the same adjusted and unadjusted analyses for each of the stores: see Table 4 for the results.

Table 4: Adjusted and unadjusted regression coefficients of the holiday effect for the nine stores.

| Store ID | Adjusted Effect | Unadjusted Effect |
|---|---|---|
| 1 | 0.0896 | 0.0711 |
| 2 | 0.0765 | 0.0775 |
| 3 | 0.0736 | 0.0838 |
| 4 | 0.0487 | 0.0674 |
| 10 | 0.0873 | 0.1020 |
| 11 | 0.0605 | 0.0653 |
| 22 | 0.0123 | 0.0437 |
| 23 | -0.0187 | 0.0475 |
| 24 | 0.0826 | 0.0900 |

The nine observed adjusted holiday effects can be used to estimate the expected holiday effect ($\theta$) adjusted for the overtime trend. This effect, $\theta$, is not conditional on a specific store but averaged across all stores. The estimate of $\theta$, $\widehat{\theta}$=0.0569 and an estimate of its variance is 0.000154.

Suppose that unadjusted holiday effects are also available for the rest of the stores. The researcher classifies the stores into two groups. One group of stores aggregates stores with similar characteristics, and it is expected that the impact of holidays on sales numbers is the same, see Table 5. Other stores are different and it is possible that the holiday effect is different too, See Table 6.

Table 5: Unadjusted regression coefficients of the holiday effect available for the 25 stores with *correlated* sales.

| Store | Unad. Eff. | Store | Unad. Eff. | Store | Unad. Eff. |
|---|---|---|---|---|---|
| 5 | 0.1196 | 18 | 0.0711 | 29 | 0.1051 |
| 6 | 0.0705 | 19 | 0.0917 | 31 | 0.0697 |
| 8 | 0.0690 | 20 | 0.0655 | 32 | 0.0219 |
| 9 | 0.0759 | 21 | 0.0771 | 34 | 0.0757 |
| 12 | 0.1144 | 25 | 0.0302 | 35 | 0.1338 |
| 13 | 0.0490 | 26 | 0.0710 | 39 | 0.0552 |
| 14 | 0.0465 | 27 | 0.0591 | 40 | 0.0476 |
| 15 | 0.1150 | 28 | 0.1112 | 41 | 0.0416 |
| | | | | 45 | 0.0556 |

Table 6: Unadjusted regression coefficients of the holiday effect available for the 11 stores with *uncorrelated* sales.

| Store | Unad. Eff. | Store | Unad. Eff. | Store | Unad. Eff. |
|---|---|---|---|---|---|
| 33 | 0.0098 | 17 | 0.0812 | 36 | -0.0156 |
| 42 | 0.0163 | 7 | 0.1728 | 38 | -0.0165 |
| 30 | -0.0074 | 16 | 0.0956 | 44 | -0.0252 |
| 43 | 0.0010 | 37 | -0.0245 | | |

Can these two external sources of information be used to improve estimation accuracy of the the adjusted holiday effect? The answer is yes, and we will return to this illustrative example later in Section 4.

## 3. Methodology

This section presents the main statistical formulas regarding the use of external information proposed in [4, 5] (variance minimization), and [8, 17] (MSE minimization) and applies these methods to Walmart sales data.

### 3.1. Parameters and their Estimators

Let $\theta$ be a parameter of interest. In Section 2, the quantity of interest is

$$\begin{aligned}\theta &= E\left(\log\left(S\right)|w{=}w, pS{=}l_1, p2S{=}l_2, h{=}1\right)\\ &- E\left(\log\left(S\right)|w{=}w, pS{=}l_1, p2S{=}l_2, h{=}0\right),\end{aligned} \quad (1)$$

where the terms are explained in Table 2. An estimator of $\theta$ based on the nine Walmart stores from Table 4 is assumed to have no bias, $E\left(\widehat{\theta}\right){=}\theta$. Another estimator $\widetilde{\eta}$, known as external information, estimates $\eta$, which can be different from $\theta$. In Section 2,

$$\eta{=}E\left(\log\left(S\right)|h{=}1\right) - E\left(\log\left(S\right)|h{=}0\right) \quad (2)$$

is the unadjusted holiday effect. Since the data in Table 6 correspond to a different cohort of stores, the unadjusted holiday effect estimated on data from Table 6 may be a biased estimate of $\eta$ (the stores from Table 6 may not belong to the population of interest). Additional external information from Tables 5 and 6 can be converted into a two-dimensional estimate $\widetilde{\eta}{=}\left(\widetilde{\eta}_1, \widetilde{\eta}_2\right){=}\left(0.0737, 0.0261\right)$. The number 0.0737 is an unbiased estimate of $\eta$, $E\left(\widetilde{\eta}_1\right){=}\eta$. Note that Table 4 can also be used to estimate $\eta$, because the unadjusted holiday effect was also estimated for each of the nine stores, $\widehat{\eta}_1$=0.0720. The second number in $\widetilde{\eta}$ ($\widetilde{\eta}_2$=0.0261) is a possibly biased estimate of $\eta$, $E\left(\widetilde{\eta}_2\right){=}\eta{+}\delta$.

Further, we use a "hat" to denote estimators based on the main dataset and a "tilde" for additional information quantities.

### 3.2. Method

To combine external information with the main data, we use the family of estimators:

$$\theta^{\Lambda}{=}\widehat{\theta}{+}\Lambda\left(\widetilde{\eta} - \widehat{\eta}\right), \quad (3)$$

where $\Lambda$ is an unknown (possibly multidimensional) parameter. In (3), $\widehat{\eta}$ is an estimate based on the main data. Note that $E\left(\widehat{\eta}\right){=}\eta$, but $E\left(\widetilde{\eta}\right){=}\eta{+}\delta$, where $\delta$ is a *possible* bias or a vector of biases. Section 2 bias has two components and

$$\begin{aligned}\widehat{\delta} &= \widetilde{\eta} - \widehat{\eta}\\ &= \left(0.0720, 0.0720\right) - \left(0.0737, 0.0261\right)\\ &= \left(-0.0017, 0.0459\right).\end{aligned} \quad (4)$$

Following [8], minimum MSE among $\theta^{\Lambda}$ estimators is reached at

$$\theta^0\left(\delta\right){=}\widehat{\theta} - cov\left(\widehat{\theta}, \widehat{\delta}\right) E^{-1}\left(\widehat{\delta}\widehat{\delta}^T\right)\widehat{\delta}^T \quad (5)$$

and

$$MSE\left(\theta^0\right){=}cov\left(\widehat{\theta}\right) - cov\left(\widehat{\theta}, \widehat{\delta}\right) E^{-1}\left(\widehat{\delta}\widehat{\delta}^T\right) cov\left(\widehat{\delta}, \widehat{\theta}\right),$$

where $E\left(\widehat{\delta}\widehat{\delta}^T\right){=}cov\left(\widehat{\eta}\right){+}cov\left(\widetilde{\eta}\right){+}\delta\delta^T$ and "$cov\left(\cdot\right)$" is a variance-covariance matrix.

The special case of $\delta$=0 makes $\theta^{\Lambda}$ unbiased. Then,

$$\theta^0(0) = \widehat{\theta} - cov\left(\widehat{\theta},\widehat{\delta}\right) cov^{-1}\left(\widehat{\delta}\right)\widehat{\delta}^T \tag{6}$$

achieves minimal variance in $\theta^{\Lambda}$, see [4]; $T$ denotes transposition. Then

$$\begin{aligned} cov\left(\theta^0(0)\right) &= cov\left(\widehat{\theta}\right) \\ &- cov\left(\widehat{\theta},\widehat{\delta}\right) cov^{-1}\left(\widehat{\delta}\right) cov\left(\widehat{\delta},\widehat{\theta}\right). \end{aligned} \tag{7}$$

For a one-dimensional case, the quadratic form in Equation (7) is

$$M = cov\left(\widehat{\theta},\widehat{\delta}\right) cov^{-1}\left(\widehat{\delta}\right) cov\left(\widehat{\delta},\widehat{\theta}\right) \geq 0.$$

- If $\widehat{\theta}$ and $\widehat{\delta}$ are uncorrelated, $M$=0 and $\theta^0(\delta) = \widehat{\theta}\ \forall\eta$.
- If $cov\left(\widehat{\theta},\widehat{\delta}\right) = cov\left(\widehat{\theta}\right)$ $(\eta=\theta)$, $M = cov\left(\widehat{\theta}\right)$, $\theta^0(0) = \theta$ and $cov\left(\theta^0(0)\right) = 0$.

The estimator $\theta^0(\delta)$ needs covariances to be applicable in practice. Plus, $\delta$ is also unknown. Dmitriev and his colleagues [10] used the same family of estimators. They assumed $\widetilde{\eta} = \eta + \delta$ belongs to a pre-determined set of values.

We use the main data to estimate unknown quantities in $\theta^0(\delta)$:

$$\widehat{\theta}^0(\delta) = \widehat{\theta} - \widehat{cov}\left(\widehat{\theta},\widehat{\delta}\right)\left(\widehat{cov}(\widehat{\eta}) + \widehat{cov}(\widetilde{\eta}) + \delta\delta^T\right)^{-1}\widehat{\delta}^T. \tag{8}$$

### 3.3. Large sample properties

Let $\theta$ and $\eta$ be scalar quantities. Under certain regularity conditions

$$\sqrt{n}\left(\widehat{\theta}^0(\delta) - \theta^0(\delta)\right) = o_p(1). \tag{9}$$

Consequently, $\forall$ fixed $\delta \neq 0$,

$$\sqrt{n}\left(\theta^0(\delta) - \theta\right) = o_p(1) \tag{10}$$

and

$$\sqrt{n}\left(\widehat{\theta}^0(\delta) - \theta\right) = o_p(1). \tag{11}$$

From (10) and (11)

$$\sqrt{n}\left(\widehat{\theta}^0(\delta) - \theta^0(\delta)\right) = o_p(1). \tag{12}$$

Estimator $\widehat{\theta}^0(\delta)$ still cannot be used in practice because $\delta$ is know known. The use $\widehat{\delta}$ leads to

$$\widehat{\theta}^0\left(\widehat{\delta}\right) = \widehat{\theta} - \widehat{cov}\left(\widehat{\theta},\widehat{\delta}\right)\left(\widehat{cov}(\widehat{\eta}) + \widehat{cov}(\widetilde{\eta}) + \widehat{\delta}\widehat{\delta}^T\right)^{-1}\widehat{\delta}^T. \tag{13}$$

The application of $\widehat{\delta}$ instead of $\delta$ makes (9) invalid: if $\delta$=0, $\sqrt{n}\left(\widehat{\theta}^0\left(\widehat{\delta}\right) - \theta^0(0)\right) = O_p(1)$, which means that $\sqrt{n}\left(\widehat{\theta}^0\left(\widehat{\delta}\right) - \theta^0(0)\right)$ does not go to zero, in probability.

Let $\delta = \delta_1\sqrt{n}$, where $\delta_1 \in (-\infty, +\infty)$ is a local alternative, $n$ denote the sample size of the empirical data set available to the data analyst, and $m$ be the size of the dataset used to obtain additional information. For the analysis of asymptotic properties we will tie these two sample sizes asymptotically with $\frac{n}{m} \to k$, where $k$ is a non-negative real number or a $+\infty$. We assume that the estimators based on empirical and external data are regular enough so that the law of large numbers applies:

$$K_{\theta,\eta} = \lim_{n\to\infty} n\cdot\widehat{cov}\left(\widehat{\theta},\widehat{\delta}\right) = \lim_{n\to\infty} n\cdot\widehat{cov}\left(\widehat{\theta},\widehat{\eta}\right),$$

$$K_{\eta,\eta} = \lim_{n\to\infty} n\cdot\widehat{cov}\left(\widehat{\eta}\right),$$

$$K_{\theta,\theta} = \lim_{n\to\infty} n\cdot\widehat{cov}\left(\widehat{\theta}\right),$$

and

$$K'_{\eta,\eta} = \lim_{m\to\infty} m\cdot\widetilde{cov}\left(\widetilde{\eta}\right)$$

are constants (asymptotic covariances). We will also assume that a central limit theorem applies so that

$$\xi_\theta = N(0, K_{\theta,\theta}) = \lim_{n\to\infty}\sqrt{n}\left(\widehat{\theta} - \theta\right),$$

$$\xi_\eta = N\left(0, K_{\eta,\eta}\right) = \lim_{n\to\infty}\sqrt{n}\left(\widehat{\eta} - \eta\right),$$

$$\xi'_\eta = N\left(0, K'_{\eta,\eta}\right) = \lim_{m\to\infty}\sqrt{m}\left(\widetilde{\eta} - \eta\right),$$

and, consequently,

$$\begin{aligned} \xi_\delta &= \lim_{n\to\infty}\sqrt{n}\left(\widehat{\delta} - \delta\right) \\ &= \lim_{n\to\infty}\sqrt{n}\left(\widehat{\eta} - \eta\right) \\ &- \sqrt{k}\lim_{m\to\infty}\sqrt{m}\left(\widetilde{\eta} - \eta - \delta_1\sqrt{m}\right) \\ &= N\left(\delta_1, K_{\eta,\eta} + kK'_{\eta,\eta}\right). \end{aligned} \tag{14}$$

The random variable $\xi_\delta$ can be represented as $\xi_\delta = \xi_\eta + \sqrt{k}\xi_{\eta'}$, which shows that $\xi_\delta$ and $\xi_\theta$ can be correlated because $\xi_\theta$ and $\xi_\eta$ are based on the same dataset.

Thus, the asymptotic behaviour of $\widehat{\theta}^0\left(\widehat{\delta}\right)$ differs from a normal distribution. Then the non-normal asymptotic behavior for large samples is

$$\begin{aligned} &\sqrt{n}\left(\widehat{\theta}^0\left(\widehat{\delta}\right) - \theta\right) = \sqrt{n}\left(\widehat{\theta} - \theta\right) \\ &- n\cdot\widehat{cov}\left(\widehat{\theta},\widehat{\delta}\right)[n\cdot\widehat{cov}(\widehat{\eta}) \\ &+ n\cdot\widehat{cov}(\widetilde{\eta}) + n\cdot\widehat{\delta}\widehat{\delta}^T]^{-1}\sqrt{n}\cdot\widehat{\delta} \\ &\xrightarrow{d} \xi_\theta - K_{\theta,\eta}\left(K_{\eta,\eta} + kK'_{\eta,\eta} + \xi_\delta^2\right)^{-1}\xi_\delta. \end{aligned} \tag{15}$$

The above asymptotic behaviour depends on two (dependent) normal random variables $\xi_\delta\left(=\sqrt{n}\left(\widehat{\theta} - \theta\right)\right)$ and $\xi_\theta\left(=\sqrt{n}\cdot\widehat{\delta}\right)$.

Overall, if $\delta$=0 can be surely assumed, the minimum variance estimator $\widehat{\theta}^0(0)$ is to be used, and if some protection against possible bias (disinformation/misinformation) is needed then minimum MSE estimation with $\widehat{\theta}^0\left(\widehat{\delta}\right)$ is a better choice with the understanding that $\widehat{\theta}^0\left(\widehat{\delta}\right)$ is inferior to $\widehat{\theta}^0(0)$ under $\delta$=0. The large sample distribution of $\widehat{\theta}^0\left(\widehat{\delta}\right)$ differs from normal, but is known, see (15). The estimator $\widehat{\theta}^0(\delta)$ can be used to evaluate the impact of bias on the estimating procedure.

### 3.4. A Monte-Carlo simulation study comparing minimum variance and minimum MSE estimation

To illustrate large sample properties of minimum variance and minimum MSE approaches, we have performed a Monte-Carlo experiment with 500,000 repetitions. The statistical model generated two samples: (1) the empirical sample, which is a sample with 100 paired standard normal random variables ($X_1$ and $Y_1$) with $cor(X_1, Y_1)$=0.9 and (2) the external sample with 1000 standard normal random variables ($X_2$). The objective is to estimate the mean of $Y$, which is equal to zero in this example.

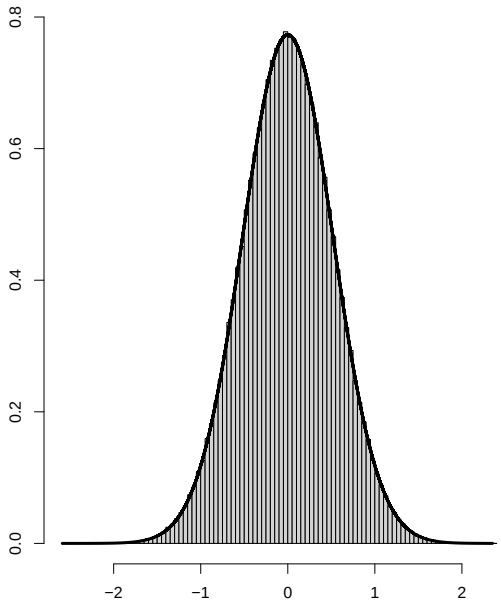


Figure 2: Histogram and a normal approximation of the distribution of $\sqrt{100}\widehat{\theta^0}(0)$, see Section 3.4; 500,000 Monte-Carlo simulations.

The asymptotic distribution of $\widehat{\theta}$ (mean of $Y_1$) is approximately normal, so that $\sqrt{100}\cdot\widehat{\theta} \sim N(0,1)$ leading to the width of 95% for $\sqrt{100}\cdot\widehat{\theta}$ equal to 3.92 (=2 · 1.96). The asymptotic distribution of $\sqrt{100}\cdot\widehat{\theta^0}(0)$ is also approximately normal with mean =0 and variance =0.266358, see Figure 2. The distance between 2.5% and 97.5% level quantiles of the distribution of $\sqrt{100}\cdot\widehat{\theta^0}(0)$ is equal to 2.03227. Wald's confidence interval ("mean estimate" ±1.96 "standard deviation of the estimate") had an almost identical length (=2.023107).

The asymptotic distribution of $\sqrt{100}\cdot\widehat{\theta^0}\left(\widehat{\delta}\right)$ is not normal anymore and is shown in Figure 3. The normal approximation allows us to visually evaluate the departure from normality. The absence of asymptotic normality, however, is not really a problem. Since the asymptotic distribution is known it still can be used for estimation, hypothesis testing, and for calculating confidence intervals. For example, the distance between the 2.5% and 97.5% level quantiles of the distribution of $\sqrt{100}\cdot\widehat{\theta^0}\left(\widehat{\delta}\right)$ is equal to 3.20191. Wald's confidence interval has a shorter length (=3.064861) associated with a less than 95% coverage.

This Monte-Carlo study demonstrates that if a data analyst is confident that additional information on an auxiliary variable is unbiased, then additional information should be incorporated using minimum variance estimation. If, however, the additional information may be biased, minimum MSE is a more appropriate method.

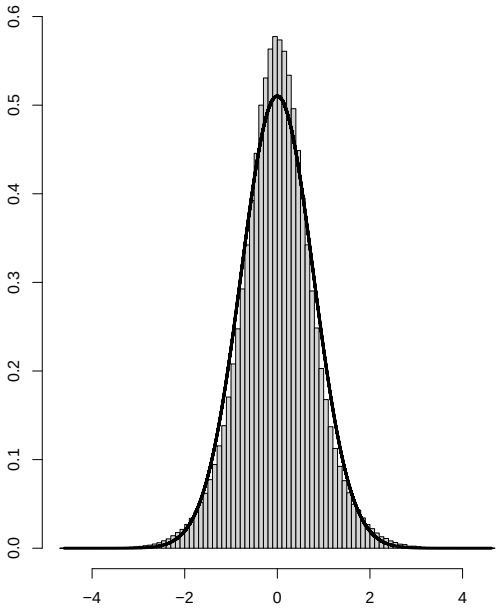


Figure 3: Histogram and a normal approximation of the distribution of $\sqrt{100}\widehat{\theta^0}\left(\widehat{\delta}\right)$, see Section 3.4; 500,000 Monte-Carlo simulations.

## 4. Illustrative Example

Section 3 shows that the minimum variance estimator $\widehat{\theta^0}(0)$ and the minimum MSE estimator $\widehat{\theta^0}\left(\widehat{\delta}\right)$ are the estimators to use in practice. In this section, we show how to apply these formulas to the adjusted holiday effect estimation. R code for this section is added to Appendix 6.

Suppose, vectors $X_1$ and $Y_1$ contain unadjusted and adjusted holiday effects from Table 4, $X_2$ keeps unadjusted holiday effects of similar stores given in Table 5, and $X_3$ keeps unadjusted holiday effects for other Walmart sores.

The correlation between $X_1$ and $Y_1$ is 84.8% which indicates that external information in $X_2$ and possibly in $X_3$ could be useful for estimating $EY$=$\theta$ .

Using empirical $X_1$ and $Y_1$ data we obtain $\widehat{\theta}$=0.05693, $\widehat{Var}\left(\widehat{\theta}\right)$=0.000154, $\widehat{\eta}$=0.072045, $\widehat{Var}\left(\widehat{\eta}\right)$=0.000040, $\widehat{Cov}\left(\widehat{\theta},\widehat{\eta}\right)$=0.000066 and $\widehat{Cor}\left(\widehat{\theta},\widehat{\eta}\right)$=0.847723. Unbiased additional information available in $X_2$ is summarized by $\widetilde{\eta}_1$=0.07372 and $\widehat{Var}(\widetilde{\eta}_1)$=0.000034. Possibly biased additional information available in $X_3$ is summarized by $\widetilde{\eta}_2$=0.026117 and $\widehat{Var}(\widetilde{\eta}_2)$=0.000366.

### 4.1. Using Unbiased Additional Information

If the additional information is $\widetilde{\eta}_1$ and $\widetilde{Var}(\widetilde{\eta}_1)$, then the estimator using this unbiased information is $\widehat{\theta}^0(0)$=0.058436 and its variance is $\widehat{Var}\left(\widehat{\theta}^0(0)\right)$=0.000095.

The estimator $\widehat{\theta}^0(0)$ asymptotically secures the smallest variance in the class of unbiased estimators $\theta^\Lambda$. The estimated variance of $\widehat{\theta}^0(0)$ is 61.3% of variance of $\widehat{\theta}$; 38.7% reduction in variance. The estimated standard deviation (SD) of $\widehat{\theta}^0(0)$ is 0.009726 $\left(=\sqrt{0.000095}\right)$, the estimated SD of $\widehat{\theta}$ is 0.01242 $\left(=\sqrt{0.000154}\right)$. Then, the ratio of the SDs = 0.7830974, which means that the width of the confidence interval is reduced by 21.7%.

### 4.2. Using Possibly Biased Additional Information

The value $\widetilde{\eta}_2$=0.026117 is possibly a biased estimator of $\eta$. Then, the minimum mean squared error estimator $\widehat{\theta}^0\left(\widehat{\delta}\right)$=0.055718 shows a very small shift from $\widehat{\theta}$=0.056930, but the MSE showed almost no change: 0.000153 and 0.000154. The square roots of these MSEs (RMSEs) are: 0.012349 and 0.01242 for $\widehat{\theta}^0\left(\widehat{\delta}\right)$ and $\widehat{\theta}$, respectively. This corresponds to just a 0.57% reduction of the RMSE. This example indicates that the use of additional information from $X_3$ has been suppressed by the squared bias: $\widehat{\delta}^2=(\widehat{\eta}-\widetilde{\eta}_2)^2=(0.072045-0.026117)^2=0.002109$.

Another example of using possibly biased information is applying minimum MSE estimation to the additional information $\widetilde{\eta}_1$ considered in Section 4.1 under the unbiasedness assumption. Then, the new estimator and its MSE are 0.058381 and 0.000097, respectively.

This new estimator and its MSE are almost identical to the estimator with the use of unbiased information and its variance calculated in Section 4.1: the difference is only observed in the sixth decimal [this is why we kept to six decimals in this report].

## 5. Summary

Additional information available from external sources in the form of estimated statistical quantities [such as means, regression coefficients, etc.] and their variances can improve statistical inference. This manuscript shows how such additional information can be incorporated in statistical estimation. The illustrative example using Walmart sales data shows how the estimation of an adjusted effect of holiday sales can be done with higher accuracy when relevant additional information is properly used.

A multiple linear regression model with log-transformed Walmart weekly sales was selected mostly for illustrative purposes. There are many other statistical models which can be used for fitting sales data– the chosen regression model may not be the best one. We have pragmatically used multiple linear regression with logarithmic transformation of weekly sales to make linear models applicable for the Walmart sales data. The statistical theory reported in this manuscript only needs asymptotic normality of estimators, and regression coefficients in this linear regression model certainly satisfy this requirement.

The illustrative example shows that this information can be available in two forms: unbiased and possibly unbiased. If additional information deliberately altered (falsified) the data then the variance minimization may not be appropriate. In this case, minimization of mean squared error detects that the additional information is not consistent with the main dataset, and the effect of additional information is reduced. If the external information does not contradict the main data, the minimum variance estimator outperforms the minimum mean squared error approach, but the protection against bias is not guaranteed.

What about other approaches? Meta-analysis combines estimators from multiple data sources (see for example [18]), which is also our strategy. However, meta-analysis cannot combine estimates on different quantities. For example, our main interest is in an *adjusted* holiday effect, but external information only provides estimates of an *unadjusted* holiday effect. Meta-analysis would require the same adjusted holiday effect to be available from multiple data sources. Our statistical methodology allows us to incorporate estimates of different quantities, as illustrated with the use of an unadjusted effect available from an external dataset. This makes our approach distinctly different.

To the best of the authors' knowledge, there are no existing frequentist statistical methods for incorporating uncertain correlated additional information, except for the MMSE and MVAR considered in this manuscript. There are, however, several Bayesian statistical methods which naturally allow the incorporation of uncertain additional information. Recently, MMSE and MVAR methods along with three Bayesian methods on the use of external additional information were applied to the same data, but no formal comparisons between the methods were completed [19].

Overall, we encourage data analysts to be open to the possibility of using additional information when available.

## References

[1] R. H. Hayes, "Statistical estimation problems in inventory control", *Manag. Sci.*, vol. 15, no. 11, pp. 686–701, 1969.

[2] Z.-P. Fan, Y.-J. Che, Z.-Y. Chen, "Product sales forecasting using online reviews and historical sales data: A method combining the bass model and sentiment analysis", *Journal of Business Research*, vol. 74, pp. 90–100, 2017.

[3] L. H. Liyanagea, J. Shanthikumar, "Apractical inventory control policy using operational statistics", *Oper. Res. Lett.*, , no. 33, pp. 341–348, 2005.

[4] S. Tarima, D. Pavlov, "Using auxiliary information in statistical function estimation", *ESAIM: Probab. Stat.*, vol. 10, pp. 11–23, 2006.

[5] S. Tarima, S. Slavova, T. Fritsch, L. Hall, "Probability estimation when some observations are grouped", *Stat. Med.*, vol. 26, no. 8, pp. 1745–1761, 2007.

[6] M. Albertus, "Asymptotic z and chi-squared tests with auxiliary information", *Metrika*, vol. XX, pp. xx–xx, 2022.

[7] S. Tarima, K. Patel, R. Sparapani, M. O'Brien, L. Cassidy, J. Meurer, "Use of previously published data in statistical estimation", "International Conference on Risk Analysis", pp. 78–88, Springer, 2022.

[8] S. Tarima, Y. Dmitriev, "Statistical estimation with possibly incorrect model assumptions", *Bul. Tomsk St. University: cont., comput., inf.*, vol. 8, pp. 78–99, 2009.

[9] S. Tarima, A. Vexler, S. Singh, "Robust mean estimation under a possibly incorrect log-normality assumption", *Commun. Stat.–Simul. C.*, vol. 42, no. 2, pp. 316–326, 2013.

[10] Y. Dmitriev, P. Tarassenko, Y. Ustinov, "On estimation of linear functional by utilizing a prior guess", A. Dudin, A. Nazarov, R. Yakupov, A. Gortsev, eds., "Information Technologies and Mathematical Modelling", pp. 82–90, Springer International Publishing, Cham, 2014.

[11] Y. Dmitriev, G. Koshkin, V. Lukov, "Combined identification and prediction algorithms", "IV International Research Conference: Information Technologies in Science, Management, Social Sphere and Medicine", pp. 244–247, Tomsk, December, 2017.

[12] Z. Zenkova, E. Krainova, "Estimating the net premium using additional information about a quantile of the cumulative distribution function", *Bus. Inform.*, vol. 42, no. 4, pp. 55–63, 2017, doi: 10.17323/1998-0663.2017.4.55.63.

[13] S. Tarima, Z. Zenkova, "Use of uncertain additional information in newsvendor models", "2020 5th International Conference on Logistics Operations Management (GOL)", pp. 1–6, IEEE, 2020.

[14] R Core Team, *R: A Language and Environment for Statistical Computing*, R Foundation for Statistical Computing, Vienna, Austria, 2021.

[15] N. Stojanović, M. Soldatović, M. Milićević, "Walmart recruiting–store sales forecasting", "Proceedings of the XIV International Symposium Symorg", p. 135, 2014.

[16] C. Catal, E. Kaan, B. Arslan, A. Akbulut, "Benchmarking of regression algorithms and time series analysis techniques for sales forecasting", *Balkan Journal of Electrical and Computer Engineering*, vol. 7, no. 1, pp. 20–26, 2019.

[17] S. Tarima, B. Tuyishimire, R. Sparapani, L. Rein, J. Meurer, "Estimation combining unbiased and possibly biased estimators", *Journal of Statistical Theory and Practice*, vol. 14, no. 2, pp. 1–20, 2020.

[18] J. P. Higgins, J. Thomas, J. Chandler, M. Cumpston, T. Li, M. J. Page, V. A. Welch, "Cochrane handbook for systematic reviews of interventions version 6.2 (updated february 2021)", https://www.training.cochrane.org/handbook.

[19] S. Calderazzo, S. Tarima, C. Reid, N. Flournoy, T. Friede, N. Geller, J. L. Rosenberger, N. Stallard, M. Ursino, M. Vandemeulebroecke, K. Van Lancker, S. Zohar, "Coping with information loss and the use of auxiliary sources of data: A report from the niss ingram olkin forum series on unplanned clinical trial disruptions", 2022, doi:10.48550/ARXIV.2206.11238.



## 6. Appendix: R code

```
> X1
[1] 0.07110327 0.07749012 0.08376658
[4] 0.06740423 0.10202317 0.06534485
[7] 0.04374566 0.04748405 0.09003966
> Y1
[1]  0.08962477  0.07652780  0.07355976
[4]  0.04872447  0.08732017  0.06047420
[7]  0.01231537 -0.01873908  0.08256086
> X2
[1] 0.11962485 0.07054883 0.06895547
[4] 0.07593105 0.11436723 0.04902411
[7] 0.04647529 0.11497511 0.07109170
[10] 0.09170929 0.06551585 0.07711085
[13] 0.03021001 0.07095118 0.05911399
[16] 0.11120773 0.10513213 0.06966771
[19] 0.02192388 0.07565785 0.13377096
[22] 0.05518881 0.04764482 0.04162753
[25] 0.05558277
> X3
[1] 0.009760383  0.016252703 -0.007369093
[4] 0.000954928  0.081232011  0.172753274
[7] 0.095586385 -0.024469670 -0.015618603
[10] -0.016530748 -0.025266635

> (n <- length(X1))
[1] 9
> (m1 <- length(X2))
[1] 25
> (m2 <- length(X3))
[1] 11
> round(mX1 <- mean(X1),6)
[1] 0.072045
> round(vX1 <- var(X1)/n,6)
[1] 0.000040
> round(mY1 <- mean(Y1),6)
[1] 0.056930
> round(vY1 <- var(Y1)/n,6)
[1] 0.000154
> round(corX1Y2 <- cor(X1,Y1),6)
[1] 0.847723
> round(covX1Y2 <- cov(X1,Y1)/n,6)
[1] 0.000066
> round(mX2 <- mean(X2)/m1,6)
[1] 0.07372
> round(vX2 <- var(X2)/m1,6)
[1] 0.000034
> round(mX3 <- mean(X3),6)
[1] 0.026117
> round(vX3 <- var(X3)/m2,6)
[1] 0.000366

> round(mY1 - (covX1Y2) /(vX1+vX2) *
(mX1-mX2),6)
[1] 0.058436
> round(vY1 - (covX1Y2^2)/(vX1+vX2),6)
[1] 0.000095

> round(mY1 - (covX1Y2 /(vX1 + vX3 +
(mX1 - mX3)^2)) * (mX1-mX3),6)
[1] 0.055718
> round(vY1 - (covX1Y2^2 /(vX1 + vX3 +
(mX1 - mX3)^2)),6)
[1] 0.000153

> round(mY1 - (covX1Y2 /(vX1 + vX2 +
(mX1 - mX2)^2)) * (mX1-mX2),6)
[1] 0.058381
> round(vY1 - (covX1Y2^2 /(vX1 + vX2 +
(mX1 - mX2)^2)),6)
[1] 0.000097
```

JENRS

Received: 20 March 2022, Revised: 25 June 2022, Accepted: 31 July 2022, Online: 19 August 2022

DOI: https://dx.doi.org/10.55708/js0108003

# Magneto-Optical Waveguide Logic Gates and their Applications

**Shukhrat Egamov *, Abduvali Khidirov, Mirzokulov Khotam Bakhtiyor ugli**

Tashkent University of Information Technologies, Samarkand Branch, Samarkand, 140100, Uzbekistan
* Corresponding author: Shukhrat Egamov, Samarkand, 140037, Uzbekistan, Email: s_egamov@mail.ru
ORCID Author 1: 0000-0002-3454-6867, ORCID Author 2: 0000-0001-8146-3987, ORCID Author 3: 0000-0003-1236-5464

**ABSTRACT:** The results of studying the possibilities of the properties of magneto-optical qubits obtained using the Faraday rotation effect are presented. Waveguide geometries have been chosen for the design of various information processing and transmission devices based on new concepts creating key elements of logic gates, with new architectures applicable to different fields of science and industry. A mechanism for controlling magneto-optical qubits could be implemented for modeling of several magneto optical logic elements in waveguide forms, including simultaneous parallel *AND, XOR* and other procedures The proposed device can be used to create a wide range of information processing and transmission components founded on new strategies.

**KEYWORDS:** Faraday rotation, Magneto optical waveguide, Magneto optical qubits, Logic gates

## 1. Introduction

Today, cyberspace is becoming a hub of the most advanced successes and approaches of modern technology. In the virtual world, it is no longer possible to process terabytes of data with ordinary computers and supercomputers. Therefore, countries around the world are actively researching the use of new strategies to develop quantum computing and artificial intelligence systems.

Quantum information processing has fundamental advantages in the fields of computing, communication security and ultra-precise measurements, but ways to make real devices are still being explored.

In this article, we present the results of the prospective study of applying the properties of magneto optical (MO) qubits in different fields of science and technology, and the design of various applications for processing according to new principles using logic elements with new architectures, devices that store and transmit information.

Main objective of this work is to present main properties of logic gates created using magneto-optical (MO) features of photons appearing in organic Plexiglas waveguide with a reasonable Verdet constant in the visible range influenced by external magnetic field. The logic *XOR* and *AND* operations are performed simultaneously in a same waveguide and can be detected with minimal peripheral electronics. Operation of the waveguide MO half adder (HA) was studied experimentally by means of the magnetic field modulation given by a low-frequency generator. *XOR* and *AND* logic operations are created to obtain *Carry out* and *Sum* outputs on separate channels using waveguide *X* geometry. Variety of designed magneto optical logic gates can be directly applied for fiber optics communication purposes in future as a tool for processing and transmitting information.

## 2. Faraday Rotation and Magneto-Optical Qubits

The development of quantum information management capabilities requires high quality control of the propagation trajectory and interference of qubits with polarization encoding of photons, which are used to process and transmit information. These conditions can be implemented much more easily with the help of microminiaturization of the classical optical architecture, switching to the use of 3-D and 2-D configurations of optical (and, accordingly, magneto-optical) waveguides with appropriate transparency windows [1-3].

The magneto optical Faraday effect was chosen as the main foundation for creating the magneto-optical qubits, observing their evolution, and recording interactions in an optical waveguide. The Faraday effect, like the vast majority of other magneto-optical phenomena, arises essentially as a consequence of the Zeeman effect and is associated with the features of the polarization characteristics of Zeeman optical transitions and with the laws governing the propagation of polarized light in a medium with dispersion. [4-6]. The specificity of magneto-

optical effects is that in a magnetic field, in addition to the usual linear optical anisotropy, which represents itself in a medium under the action of an electric field or deformation, circular anisotropy arises associated with the nonequivalence of two directions of rotation in a plane perpendicular to the field. This important circumstance is a consequence of the axiality of the magnetic field.

Consider the propagation of linearly polarized light along the field. First of all, we note that linearly polarized light can be represented as a superposition of left-handed and right-handed circularly polarized waves, with both polarizations existing simultaneously with the same probability (Figure 1).

If light propagation through the MO material coincides with the direction of the applied field $H$, then a circular magnetic birefringence which is called the Faraday effect is observed, The Faraday effect for a given frequency of incident light is given by

$$\alpha_F = rdH \qquad (1)$$

where $\alpha_F$ is the Faraday rotation angle of the polarization plane, $r$ is a characteristic of the substance and a function of the wavelength, $d$ is the length of sample, $H$ is the external magnetic field [6]. When the field direction is changing $\alpha_F$ sign also changes to the opposite, i.e. the Faraday effect is odd in magnetization.

The simplest way to measure the Faraday rotation angle of the incident light's polarization is shown in Figure 1a. If no magnetic field is applied, the observer sees a dark field when the polarizer *PL* and analyzer *AN* are crossed (their axes are mutually orthogonal). If a magnetic field is applied to the sample, then the viewing field becomes clear.

The dark field can be obtained again by turning the analyzer clockwise or counterclockwise, depending on the applied magnetic field along or against the direction of light propagation. In the absence of a field and crossed polarizer *PL* and analyzer *AN*, we observe a blackout in the observer's view field at the exit. When the magnetic field is active (Figure 1a), the plane of light polarization rotates and in order to obtain darkening again, it is necessary to turn the analyzer by some angle to the right, which will be equal to the Faraday angle $\alpha_F$. When changing the direction of the magnetic field we get a left rotation, that is, counterclockwise.

To measure the Faraday rotation by the modulation photometric method, is chosen geometry in which the angle between the polarizer and the analyzer is set to $\pi/4$ radians, in contrast to the visual one, in which the angle between the axes *PL* and *AN* is $\pi/2$ (Figure 1b) while alternating magnetic field is applied. The modulation photometric method of measuring Faraday rotation is more convenient to check $\alpha_F$ more precisely.

We can use the MO Faraday rotation effect to build logic devices using a bulk Plexiglas waveguide that has a fairly large specific Faraday rotation and low absorption in the visible spectrum.

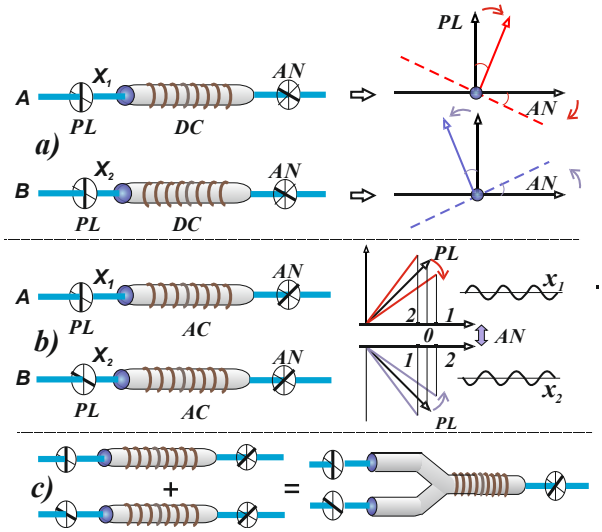


Figure 1: Observation of the Faraday effect: a) in the presence of a fixed magnetic field parallel (above) and antiparallel (below) to the direction of the incident light – right and left rotation; b) the behavior of the variable intensity component of the detected light for two orthogonal polarizations, respectively; c) combining two signals in one Y shape waveguide

A novel of MO waveguide half adder (HA) has been developed and experimentally tested. A diagram of the simplest MO HA used to test experimentally the operability of *XOR* and *AND* logic elements is shown in Figure 2. In such a geometry we were able to measure a Faraday rotation angle of about 0.25°/cm at a magnetic alternating field strength of 100 Oersted and a wavelength of 440 nm. It has been proven that by using this configuration and the appropriate electronics to measure the output signal , we can easily get a match to the truth table values for our gates without the extra switchings as in traditional electronics..

The concept of "magneto optical qubits" is presented briefly in [1]. Another option of MO qubits has been proposed in [7], where the implementation of single qubit quantum gates exploits the longitudinal and polar magneto optic Kerr effect in the reflection geometry. For longitudinal Kerr effect the magnetic field is located on planes of incident light polarization and the surface of an opaque sample.

One of the main benefits of MO qubits over optical qubits in transparent waveguides is opportunity to increase the coherence time of qubit by six or more orders of magnitude. It allows the creation of quantum computing devices models with minimized troubles. The simplest classical logic *AND*, *XOR* and *NOT* gates including HA and adders. It also opens a choice to create *C-NOT* (*Controlled NOT)* quantum gate using basic digital logic concepts.

Quantum behavior of photons formal features of one and two input signals can be described via proposed magneto optical qubit generator (MOQG) properties.

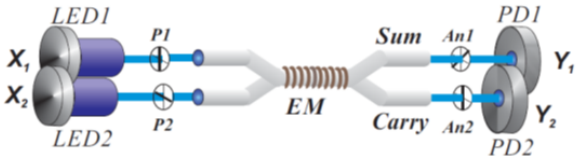


Figure 2: Schematic representation of HA (peripheral electronics not shown): *LED1* and *LED2* are light-emitting diodes ($\lambda$= *440 nm*), $X_1$ and $X_2$ signals with *HP* and *VP* light polarization orientations, *EM* is an electro-magnet; *Sum* is the summing waveguide channel; *Carry* is the transfer channel; *An1* and *An2* are analyzers; *PD1* and *PD2* are photodiodes for detecting output signals.

Suppose that signal *A* is represented by a beam of photons of a certain wavelength Therefore we can spatially separate them into two different rays with $A_x$ and $A_y$ orthogonal polarizations. This means we can get two different bits from the same photon source. If we connect these two rays together, we get a new state that can be called the bra vector |*A*>. Under the influence of an alternating magnetic field, |*A*> begins to oscillate with a declination amplitude equal to the Faraday rotation angle $\alpha_F$. As shown in the lower right corner of Figure 3, different alternating parts of the |*A*> eigenvalues can be obtained by changing the orientation of the output analyzer. It is important to note that with the help of waveguides we can easily detect AC and DC different currents, separate them and measure signals simultaneously induced in the PDs.

Suppose that the signal *A* is represented by a beam of photons with a certain wavelength. Therefore, we can spatially separate them into two distinct rays with $A_x$ and $A_y$ orthogonal polarizations. This means we can get two different bits from the same photon source. If we connect these two rays together, we get a new state that can be called the bra vector |*A*>. Under the influence of a changing magnetic field, |*A*> begins to oscillate with a declination amplitude proportional to the Faraday rotation angle $\alpha_F$. Various alternative parts of the eigenvalues |*A*> can be produced by changing output analyzer orientation, as shown in the lower right part of Figure 3. It is important to note that we can easily measure different types of DC and AC signals being induced on the PD at the same time in waveguides.

The variable part of the signal changes as a function of $sin2\pi\nu t$ ($\nu$ is the frequency of the alternating magnetic field) when the analyzer is oriented along the *X* axis ($P_x$) and accordingly as —$sin2\pi\nu t$ when the analyzer is oriented along the *Y* axis ($P_y$). The alternative component is zero when the analyzer is parallel to $A_{XY}$, i.e. oriented in the *XOY* plane at $\pi/4$ angle to the *X* or *Y* axis. This means that we can in fact propose the concept of MOQG with the geometry plotted in Figure 3. Any logical qubits containing device can be called a quantum register, which is more meaningful than a classical one. It is clear that instead of the classic bit with a value of *1* (the presence of an input signal *A*) or *0* (no signal) we can obtain a magneto optical quantum bit with values between *+1* and *—1* depending on the orientations of the analyzer at the output.

The initial state of a photon can be expressed as: polarization $\boldsymbol{p}$ index, spatial *s* index, orbital angular momentum *m* index and wavelength $\lambda$ [2, 3]. In our particular case, we can determine the photon's polarization and its spin number as $S = \pm 1$, just to define the MO quantum logic devices basic principles.

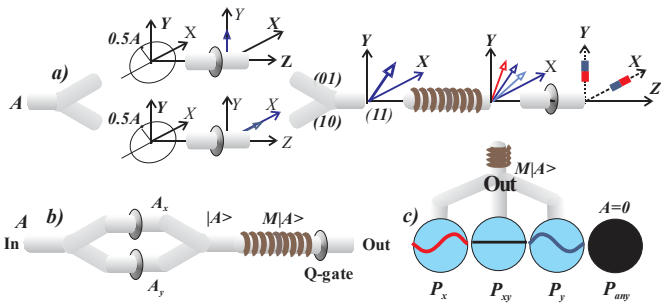


Figure 3: Processes im MOQG. a) obtaining orthogonal polarizations of MO qubits b) overall view of MOQG for one qubit, c) AC and DC signals for different orientations of output analyzers

Polaroid films (shown as discs in Figure 2) separate the incoming $X_1$ and $X_2$ optical signals into mutually orthogonal polarizations. In the upper HA channel, we get a qubit state similar to an "entangled" photon. This is expressed by the $\boldsymbol{X_1}$ and $\boldsymbol{X_2}$ vector sum just before the magnetic field is applied. The resulting angle of $\boldsymbol{y_1}$ vector between *X* and *Y* axis is equal to $\pi/4$ radians in the *XOY* plane *(Carry channel)*. Then $Y_1$ will oscillate around its initial state due to Faraday rotation during applied magnetic field.

In a *Carry out* channel the output polarizer is oriented in the *X*-direction of the passing beam polarization. When such geometry is chosen, we just register a non-zero signal if both $X_1$ *and* $X_2$ signals are generated in the *Carry out channel.* Each of $X_1$ and $X_2$ signals entering the magnetic field region due to the Faraday effect to be considered as distinct oscillating vectors in the *XOY* plane. Here we cannot operate with $\boldsymbol{A}$ and $\boldsymbol{B}$ vector sum directly because here they are not coherent.

Changes in the state of a photon (or another similar objects) can be described using operators. The waveguide branch of the "Removal" channel after the magnet coil is routed to the bottom right to the "*Sum*" channel and acts as a *CNOT* gate. Subsequently, the received MO signals are analyzed in the summation and transfer channels with properly aligned polarizers and recorded by photodetectors. Elementary calculations reveal that the truth table conditions for this model of quantum MO HA are fully satisfied, as it was in case of the classical version of MO HA.

## 3. Magneto Optical Waveguide Logic Gates

Numerical logic (Boolean algebra) deals only with binary possible numbers or two variable values that correspond to Boolean values: *0* and *1*. Thus, digital logic circuits can be functionally analyzed and synthesized using logical algebra, truth tables, and other tools that can represent a relationship between *1* and *0* while logic operations are produced [8, 9].

Boolean values of *0* or *1* are called binary numbers or bits. Set a variable with more than two values with an *n* – bits' set express 2 different values. The value of the output signal at a given point in time is called a combinatorial scheme. It is uniquely determined by the logic circuit summing the values of the input signal without data storage digital circuits [9].

These circuits can be fully described by a data sheet listing all combinations of input signals and their corresponding output values in a form of truth table. Note that a useful theorem has been proved in logical algebra: any logical function can be represented by a superposition of three functions: logical addition or disjunction *(OR)*, logical multiplication or conjunction *(AND)*, and negatiion (*NO*).

Just three basic schemes that implement the *AND*, *OR* and *NOT* functions are sufficient to construct any combination scheme. Figure 4 shows the logic gate flags above and the corresponding truth tables. Truth tables for above operations are expandable to any number of inputs. The functions performed by the schema are defined as follows:

If all inputs are *1*, *AND* element produce only *1* at output. Logical function performed by *AND:*

$$Y = X_1 \bullet X_2 \bullet \ldots \bullet X_m. \quad (2)$$

If at least in one of the electronic inputs *1* is presented *OR* circuit at the output generates only *1*. The logical function performed by the OR element:

$$Y = X_1 + X_2 + \ldots + X_m. \quad (3)$$

If logic *NO* operation is applied than output signal value will be inverted in regard to input one. Ones ttransform to zeros and vice versa. *NO* logic element (inverter) is indicated as: $Y = \overline{X}$. Consider another way to build gates that are coded and directly compatible with data transmission via fiber optic lines of communications. We are able to use the MO Faraday effect to realize various logic widgets with organic compound such as Plexiglas waveguides, which have good transparency and sufficiently big specific Faraday rotation [1, 4].

The classic HA consists of two inputs with $X_1$ and $X_2$ signals and two outputs where sum channel $Y_1$ *(Sum)* and transmission channel $Y_2$ *(Carry)* including a truth tables are presented in Figure 5.

The key element that are used as the MO waveguide is a Plexiglas sample that prevents light from absorption and scattering losses during propagation. The electromagnet is a multilayer copper wired coil.

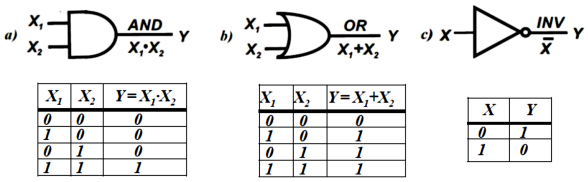


| $X_1$ | $X_2$ | $Y=X_1 \cdot X_2$ |
|---|---|---|
| 0 | 0 | 0 |
| 1 | 0 | 0 |
| 0 | 1 | 0 |
| 1 | 1 | 1 |

| $X_1$ | $X_2$ | $Y=X_1+X_2$ |
|---|---|---|
| 0 | 0 | 0 |
| 1 | 0 | 1 |
| 0 | 1 | 1 |
| 1 | 1 | 1 |

| X | Y |
|---|---|
| 0 | 1 |
| 1 | 0 |

Figure 4: Basic logic elements and their truth tables:
*a) AND; b) OR; c) NO*

Let's take a quick look at how logic gates can be designed using MO waveguides. The main purpose of the design is its operation ib modulo 2. binary counter mode. However, it has been found that a waveguide of this configuration can be adapted to operate in other modes. The functions of the remaining details needs no explanation (See Figure 2).

The basic binary coding of input signals should be done by pulse modulation of light, i.e. the *LED* comply with *ON* — "*1*", *OFF* — "*0*" during operations.

Additional explanations should be given to the physical properties of the input and output signals. The encoded data in the form of electrical signals, is converted into video pulses and transmitted to the *LEDs*, which in turn are converted into optical radiation with pulses of specific duration. These *A* and B rays are then converted to linear polarization by going through the *HP* (horizontal) and *VP* (vertical) polarizers

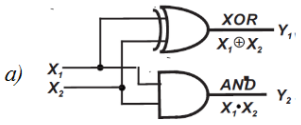


| $X_1$ | $X_2$ | $Y_1=X_1 \oplus X_2$ | $Y_2=X_1 \cdot X_2$ |
|---|---|---|---|
| 0 | 0 | 0 | 0 |
| 1 | 0 | 1 | 0 |
| 0 | 1 | 1 | 0 |
| 1 | 1 | 0 | 1 |

Figure 5: a) Symbol of the half-adder, and b) the truth table

Qubits containing logical device can be considered as a more informative quantum register compared with the classical one [6]. Now we can call them Boolean variables $X_1$ and $X_2$ or as basic vectors $|0\rangle$ and $|1\rangle$, orthogonal to each other. They pass through one or other input of the waveguide, as shown in (4) [5].

$$X_1 = \begin{pmatrix}1\\0\end{pmatrix}; \quad X_2 = \begin{pmatrix}0\\1\end{pmatrix} \quad (4)$$

Expressing a simple optical qubit as a vector in Hilbert space, for example $|0\rangle$ and $|1\rangle$ (see above: (4)), and place it in an alternating magnetic field, the spin degeneration disappears and the photon's polarization properties will change. The descriptive vector begins precession with the magnetic field frequency around the initial equilibrium state. The maximum angle of precession is proportional to the angle of Faraday rotation in the waveguide material.

To describe these forced oscillations due to Faraday effect and measure its properties it is convenient to introduce a new vector with corresponding eigenvalues. It

should be noted that the same quantum laws still applicable to these new MO "particals" as to their precursors ─ photons.

The action of the changing magnetic field leads to conversion of optical signal into magneto-optical due to the Faraday effect. Therefore, instead of the purely optical signals *X1* and *X2*, it makes sense to consider magneto optical signals that occur when entering the waveguide domain with an electromagnetic coil (Faraday domain: Figure 6).

When the magnetic field is active, the optical signals passing through the analyzer with a certainly oriented direction will get an additional intensity component. This generated variable component intensity value depends on mutual orientation of the input and output polarizers.

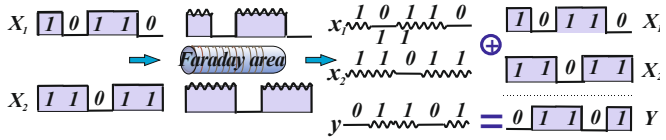


Figure 6: Development of processed signals.

The *Y* data signal captured by a photodiode are amplified and transformed into electrical *y* signals acceptable for further data processing, storage or transmission. In contrast to the classic case of an MO gate, instead of dealing with discrete *0* and *1* signals, here we are dealing with segments of sinusoids that serve as the processed signals.

It was experimentally determined that the angle of rotation of the polarization plane of the incident light at a 440 nm wavelength is about 15 min/cm while 100 Oe variable magnetic field is applied.

All possible combinations of the $X_1$ and $X_2$ input signals and relating output values summated in the *Sum* $y_1$ and *Carry y2* channels are shown in HA's truth table in Figure 5

Classic HA can be easily adjusted in combined mode without additional switching operations that are considered as follows.

The processes in the Sum and Carry channel are passing as follows [10]. Two optical signals *A* ($X_1$) and *B* ($X_2$) generated by LEDs fall into Y -shaped waveguide as shown in Figure 7. Then they pass through a polarizing filter placed between the light source and the waveguide and are converted into $X_1$ and $X_2$ signals polarized horizontally *(HP)* or vertically *(VP)* respectively. In general, entering $X_1$ and $X_2$ signals are in nature purely optical. Their electrical transformation to logic *"1"* has the order of magnitude from tens to hundreds of millivolts and expressed as potential (video) signals.

Due to the Faraday effect, the polarization plane of the transmitted light rotates in *XOY* plane to $a_F$ angle and is changed by the application of a sinusoidal alternating current to the coil. The intensity of the beam that passed throughthe analyzer is detected by the *PD1*photodiode, as shown in Figure 2.

The total detected outcoming photocurrent further can be separated into DC and AC components. The angle between polarizer and analyzer is mostly adjusted to $\pi/4$.

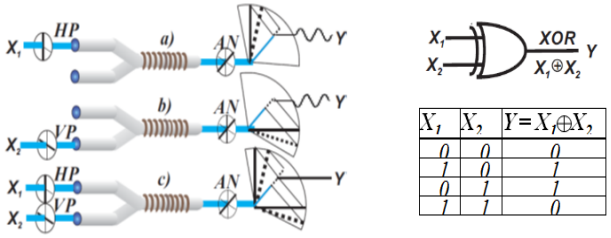


| $X_1$ | $X_2$ | $Y=X_1 \oplus X_2$ |
|---|---|---|
| 0 | 0 | 0 |
| 1 | 0 | 1 |
| 0 | 1 | 1 |
| 1 | 1 | 0 |

Figure 7: Schematic of the MO *XOR* logic element for two binary signals processing in the *Sum* waveguide channel: *a) X1 = 1, X2 = 0, Y = 1; b) X1 = 0, X2 = 1, Y = 1, c) X1 = 1, X2 = 1, Y = 0*. On the right side (from top to bottom) – symbol of *XOR* logic gate and the truth table

Let 's consider the case of $X_1$ *(HP)* and $X_2$ *(VP)* signals separately. In the absence of a magnetic field for both cases (Figures 6a and 6b) we find that the photocurrent is equal to ½ of initial beam intensity $I_0$ according to Malus' law (horizontal line on the right side of the image). The magnetic field generated in a coil leads to the Faraday rotation in the waveguide. For small values of $\alpha_F$ (Figures 7a, 7b and 7c respectively), the photocurrent depends on the material constant and variable components:

$$I_{ph}=k(I/2+I\alpha_F \sin\Omega t) \qquad (5)$$

where $k$ is the scaling factor, $I_{ph}$ is the intensity of the incident light, $\alpha_F$ is the Faraday rotation in radians, $\Omega$ is the generated magnetic field frequency, $I\alpha_F \sin\Omega t$ is the variable part of detected light intensity.

Processes taking place for different options for incomimg signals during *XOR* MO logic gate operations are displayed separately in figure 7. In this geometry the output signal *y* behavior is similar to one ib sum channel of a classic semiconductor logic circuit. Variable part of resulting intensity are represented by sinusoids. The phase difference arisen after modulation between *X1* and *X2* is equal to $\pi$ radians.

Identical to *XOR (exclusive or)* gate architecture and sinilar set of elements was chosen for the *AND* gate. The angle between the polarizer and the analyzer in this case should be adjusted to zero or $\pi/2$ radians (Figure 8).

It implies that $X_1$ and $X_2$ in the *AND* gate after the polarizers have the same polarization and similar arrangement as in Figure 7, but here the analyzer is oriented perpendicular to the $X_1$ signal polarization or parallel to $X_2$. In both cases (Figure 8a and 8b) in the presence of a signal (only $X_1$ or just $X_2$ alone), the output variable signal will be negligible.

This can be demonstrated more precisely by a simple trigonometric transformation of small Faraday rotation

angles. When both signals are present we get a sinusoidal response which can be defined as a default value of *1*.

To perform both *XOR* and operations in the same waveguide, we can switch configuration from the Y- to the X-waveguide configuration as shown in Figure 2

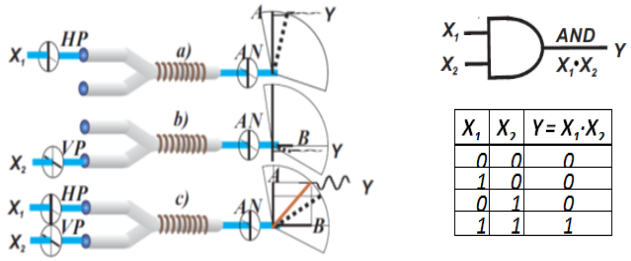


| $X_1$ | $X_2$ | $Y = X_1 \cdot X_2$ |
|---|---|---|
| 0 | 0 | 0 |
| 1 | 0 | 0 |
| 0 | 1 | 0 |
| 1 | 1 | 1 |

Figure 8: Diagram of the magneto-optical logic *AND* gate, for processing two binary signals in the *Carry out* channel: *a)* $X_1$=1, $X_2$=0, Y=0; *b)* $X_1$=0, $X_2$=1, Y=0, *c)* $X_1$=1, $X_2$=1, Y=1. On the right side from top to bottom: logic *AND* gate symbol and the truth table.

Now we will discuss some other features of the MO waveguide logic gate which seems to be very efficient for future applications.

Taking into account that there are no special designations for magneto-optical waveguides yet, it is proposed to depict them schematically as in Figure. 9b.

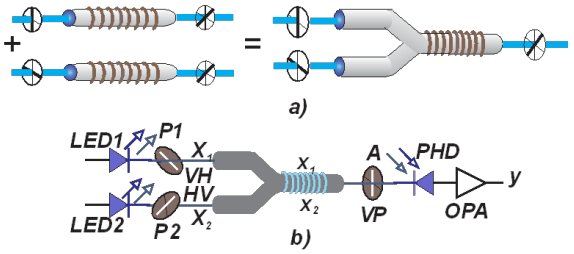


Figure 9. The main designations of the elements proposed for hybrid chips with magneto-optical logic gates. Example of the waveguide binary counter

$X_1$, $X_2$ – are input optical signals; *LED1*, *LED2* – light emitting diodes of channels *1* and *2* (inputs); *P1*, *P2* – polarizers of input channels *1* and *2* installed orthohonal to each other; *A* – output analyzer; *EM* – electromagnet-modulator; *PHD* – photodetector (silicon photodiode); Op-amp (*OPA*) – an operational amplifier or other electronics for amplifying (measuring) and fixing the output signal.

Using these notations, we will give an explanation of the *INVERTER* operation. Let's say that we want to use the device in Figure 9 to invert the binary information entering channel 1. It is assumed that binary coding is carried out using amplitude modulation, that are successive video pulses. *LED* is *ON* – "*1*", *OFF* – "*0*".

Note that the data originally encoded as an electrical signal (usually in ASCII standard) is converted into video pulses and transmitted to *LED*, which converts them into light radiation pulses

This signal then passes through the polarizer, gets *H* or *V* polarization depending on chosen geometry of the input part of the waveguide. Under the influence of the changing magnetic field, the optical signal is converted into a MO one. After passing through the analyzer, the derived output signal gets an additional variable intensity component under magnetic field influence leading to MO Faraday rotation. This signal is detected by the photodiode. Variable part of light intensity is transformed into the electrical signal, amplified and can be used further for processing or storage information.

To make the inverter work, turn on the counter in *exclusive or* mode. According to Figure 7, let $x_1$ be the input signal $y$, and the result of the inversion will be $\bar{y}$. For simplicity we have choosen the expression ***10110.*** The result of the inversion should be the expression ***01001.*** It is easy to guess that for this auxiliary channel $x_2$ must permanetly operate in the ***111111*** mode. The principle of operation of a magneto-optical inverter is clear from Figure 10

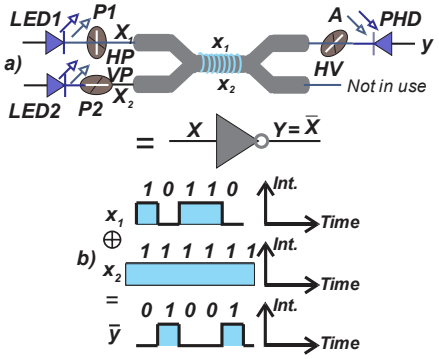


Figure 10. Magneto optical NOT logic gate *(INVERTER):* a) schematic diagram; b) time dependences of input and output signals for a magneto-optical inverter. Input signal $x_1$=*y=10110*, output signal $\bar{y}$=*01001*

The dynamic *ERASE* operation is also easily accomplished with minor changes to the configuration shown in Figure 9. To smooth the signal, it is proposed to remove the polarizer in the $x_2$ channel and leave the *LED* to work in a constant mode. The operation principle of the magneto-optical "*ERASE*" logic gate is clear from Figure 11.

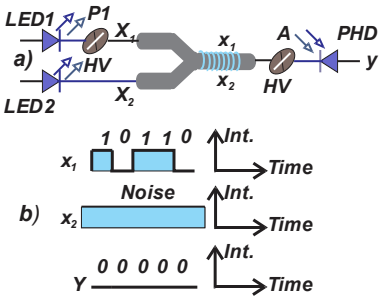


Figure 11. Dynamic magneto-optical *ERASE* logic gate*:* a) schematic diagram; b) time dependences of the input and output signals for the magneto-optical *" eraser "*. Input signal $x_1$ =*10110*, output signal *y=00000.*

The analyzer at the output of the waveguide should be installed parallel or perpendicular to the polarizer of the input channel $x_1$. In principle, in the presence of only one plane-polarized beam, the rotation of the polarization plane at the output with mutually parallel or orthogonal

orientations of the polarizer and analyzer cannot be fixed with the modulation technique, so the use of 2 channels may seem redundant. However, we take into account the fact that device parts should preferably be unified and interchangeable.

Let us now consider how the *COPY* magneto-optical gate works. To create this device, we will use the main configuration shown in Figure 9. The information signal enters as usual through the upper channel $x_1$, through the second $x_2$ the light from the constantly working *LED* passes, as in the first two cases (in *inverter* and *erase modes*).

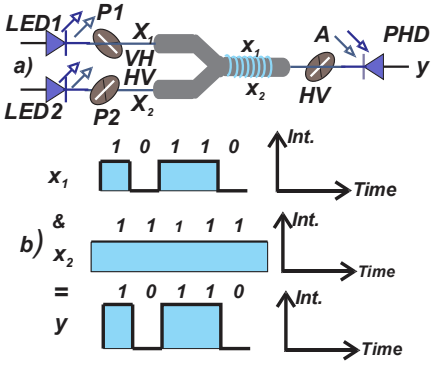


Figure 12: Dynamic magneto-optical waveguide logic gate *COPY*. a) schematic diagram; b) time dependences of the input and output signals for the magneto-optical *"copier"*. Input signal $x_1$ =10110, output signal *y=10110*

In order to be fulfilled the truth table, we apply the *AND* gate mode operation of the MO waveguide for two signals. To do this, we set the input polarizers for $x_1$ and $x_2$ mutually perpendicular to each other, and in the output channel $y$, the position of the analyzer is chosen parallel to either $x_1$ or $x_2$, that is, the geometry of the previously considered half-adder for the Carry out channel is selected.

It should be noted that these two positions of the analyzer are characterized by the fact that if the analyzer is parallel to the polarizer for channel $x_1$ and the phase shift of the output alternating signal is taken equal to zero, then when rotated by 90°, that is, when the analyzer is parallel to the polarizer $x_2$, the phase shift will be 180°. This property is used for tuning, calibration, and other ancillary operations before making accurate measurements of the Faraday effect for scientific purposes.

A schematic diagram of a hybrid magneto-optical waveguide chip assembly for use in *COPY* operations is shown in Figure 12

It is easy to see that at the output we get not only a repetition of the form and content of the input signal, but also its amplification. This circumstance will turn out to be very important, since the transmission and processing of any signal is accompanied by one or another degree of attenuation, which does not allow building a large number of cascades without noise and signal attenuation, therefore it seems that the proposed version of the *"copier"* in the future, when switching to optocoupler circuits, will be in great demand.

As for the magneto-optical waveguide *shift register*, at this stage, the options for its implementation currently are not competitive.

The fact is that for reliable functioning of above mentioned shift register, it is necessary to solve the issues of designing compatible delay lines, selecting a suitable electronic element base, adding synchronization mechanisms, etc., therefore, in this paper, the results of the study of the *shift register* are not considered.

## 4. Conclusion

The proposed quantum information processing method fundamentally changes the situation on the basic components of logic devices. Thereby we have no need for expensive bulky parts like high quality mirrors, transparent plates, crystal polarizers, phase plates, optical benches and powerful light sources. Obvious advantages of the of fiber optics and integrated optics are in fact that all processes take place in a single wave-transmitting waveguide with size of the order of a fraction of a square centimeter [11-14].

Photons with their unique properties are very convenient carrier of information. Thus they actively can be applicable for designing various logic devices based on different physical phenomena [15-18]. Photons with magnetooptical features also seems very flexible for future applcations. It makes sense to actively continue the ongoing research on the application of the results in the areas of artificial intelligence, communication technologies and cryptography.

## Conflict of Interest

The authors declare no conflict of interest.

## Acknowledgment

This work would not have been possible without the financial support of the Samarkand Branch of Tashkent University of Information Technologies and coordination with Physical Department of Samarkand State University. We are grateful to all of those

## References

[1]. S. Egamov, "Modeling of Quantum Logic Devices with the Magneto-optical Qubits Generator," in *Frontiers in Optics 2013*, I. Kang, D. Reitze, N. Alic, and D. Hagan, eds., OSA Technical Digest (online) (Optical Society of America, 2013), paper FTh1C.6.

[2]. D. Bonneau, M. Lobino, P. Jiang, C. M. Natarajan, M. Tanner, R. H. Hadfield, S. N. Dorenbos, V. Zwiller, G. Thompson, and J. L. O'Brien, "Fast path and polarization manipulation of telecom wavelength single photons in lithium niobate waveguide devices," *arXiv:1107.3476 [quant-ph]*, v1, 18 Jul. 2011.

[3]. A. Crespi, P. Mataloni, R. Ramponi, L. Samsoni, and S. Sciarrino, "Integrated optics logic gate for polarization-encoded quantum

qubits and a method for the production and use thereof," US Patent Publ. Appl. US 2014/0126030 A1, May 8, 2014.

[4]. A. K. Zvezdin and V. A. Kotov, *Magnitooptika tonkih plenok*, M.: Nauka, 1988, 192 pp. (in Russian).

[5]. K. Shinagawa, "Faraday and Kerr Effects in Ferromagnets," in *Magneto-Optics*, S. Sugano and N. Kojima, Eds. Berlin, Heidelberg: Springer, 2000, vol. 128, Springer Series in Solid-State Sciences, pp. 231-274, doi: 10.1007/978-3-662-04143-7_5.

[6]. A. K. Zvezdin and V. A. Kotov, *Modern Magnetooptics and Magnetooptical Materials*. Bristol and Philadelphia: Institute of Physics Publishing, 1997.

[7]. P. Kumar, "Single-qubit quantum gates using magneto-optic Kerr effect," *International Journal of Nuclear and Quantum Engineering*, vol. 6, no. 3, pp. 1-6, 2012.

[8]. A. L. Larin, *Fundamentals of Digital Electronics: Textbook*. Moscow: MIPT, 2008, 315 pp.

[9]. M. Predko, *Digital Electronics Demystified*. New York: McGraw-Hill, 2005, 370 pp.

[10]. Sh. Egamov, A. Khidirov, Kh. Urinov, and Kh. Zhumanov, "Waveguide Logic Gates for Magneto-optical Qubits," *Technical Physics Letters*, vol. 46, no. 10, pp. 947–949, 2020, doi: 10.1134/S1063785020100041.

[11]. P. Kok and B. W. Lovett, *Optical Quantum Information Processing*. Cambridge: Cambridge University Press, 2010, 506 pp.

[12]. M. Le Bellac, *Short Introduction to Quantum Information and Quantum Computation*. Cambridge: Cambridge University Press, 2007, 171 pp.

[13]. D. Tsiokos, E. Kehayas, K. Vyrsokinos, T. Houbavlis, L. Stampoulidis, G. T. Kanellos, N. Pleros, G. Guekos, and H. Avramopoulos, "10-Gb/s All-optical half-adder with interferometric SOA gates," *IEEE Photonics Technology Letters*, vol. 16, no. 1, pp. 284-286, Jan. 2004.

[14]. M. Lobino, P. Jiang, C. M. Natarajan, M. Tanner, R. H. Hadfield, S. N. Dorenbos, V. Zwiller, G. Thompson, and J. L. O'Brien, "Fast path and polarization manipulation of telecom wavelength single photons in lithium niobate waveguide devices," *arXiv:1107.3476 [quant-ph]*, v1, 18 Jul. 2011.

[15]. S. H. Abdulnabi and M. N. Abbas, "All-optical logic gates based on nanoring insulator-metal-insulator plasmonic waveguides at optical communication band," *Journal of Nanophotonics*, vol. 13, 016009, 2019, doi: 10.1117/1.JNP.13.016009.

[16]. M. Asghari, G. Moloudian, and M. H. Kashtiban, "A novel proposal for all-optical XOR/XNOR gate using a nonlinear photonic crystal based ring resonator," *Optica Applicata*, vol. 49, no. 2, pp. 267-276, 2019, doi: 10.5277/oa190209.

[17]. Y. Liu, F. Qin, Z.-M. Meng, F. Zhou, Q.-H. Mao, and Z.-Y. Li, "All-optical logic gates based on two-dimensional low-refractive-index nonlinear photonic crystal slabs," *Optics Express*, vol. 19, no. 3, pp. 1945-1953, 2011, doi: 10.1364/OE.19.001945.

[18]. N. H. Priya, S. Swarnakar, S. V. Krishna, et al., "Design and analysis of a photonic crystal-based all-optical 3-input OR gate for high-speed optical processing," *Optical and Quantum Electronics*, vol. 53, no. 720, 2021, doi: 10.1007/s11082-021-03374-0.



**SHUKHRAT EGAMOV** He has PhD degree in physics and mathematic from the Moscow State University. His research activity is mainly associated with Samarkand State University. Currently he is a member of Tashkent University of Information Technologies' team. He has published more than 30 articles.

**KHIDIROV ABDUVALI** has done his bachelor's degree from Tashkent University of Information Technologies in 2010. He has done his master's degree from Tashkent University of Information Technologies in 2012. More than 12 articles have been published.

**MIRZOKULOV KHOTAM** has done his bachelor's degree from Samarkand branch of Tashkent University of Information Technologies in 2014. He has done his master's degree from Tashkent University of Information Technologies in 2016. He has completed his PhD degree in technical science from the Tashkent University of Information Technologies in 2020. More than 20 articles have been published.

Received: 03 June 2022, Revised: 03 August 2022, Accepted: 16 August 2022, Online: 29 August 2022

DOI: https://dx.doi.org/10.55708/js0108004

# CRESustain: Approach to Include Sustainability and Creativity in Requirements Engineering

**Clara Silveira**[*,1], **Vitor Santos** [2], **Leonilde Reis** [3], **Henrique Mamede**[4]

[1] Scholl of Technology and Management, Polytechnic of Guarda, Guarda, 6300-559, Portugal
[2] NOVA Information Management School (NOVA IMS), Lisboa, 1070-312, Portugal
[3] School of Business Administration, Polytechnic Institute of Setúbal, Setúbal, 2914-503, Portugal
[4] INESC TEC, Universidade Aberta, Lisboa, 1269-001, Portugal

*Corresponding author: Clara Silveira, Polytechnic of Guarda, mclara@ipg.pt

**ABSTRACT:** Requirements Engineering is an evolving field facing new challenges. One of the central conundrums is sustainability in software. The possibility of using known creativity techniques while introducing the dimensions of sustainability to help provide unexpected, original, practical, and sustainable answers in software development is challenging and motivating. This paper proposes an approach, CRESustain, incorporating sustainability dimensions when introducing creativity techniques in the Requirements Engineering process. CRESustain uses various creativity techniques considered appropriate for the different stages of the RE process. It is inspired by the Sustainable Development Goals, creative problem-solving methods, and the Karlskrona Manifesto. The methodology applied to give materiality to the outcome of this work was Design Science Research, a research paradigm that uses knowledge to solve problems, generate new knowledge and insights, and results in an artefact. The main results indicate that the approach stimulates discussion about sustainability in technical, economic, social, human, and environmental dimensions focusing on the Sustainable Development Goals and people's needs.

**KEYWORDS:** Creativity, Requirements Engineering, Sustainability, Sustainable Development Goals

## 1. Introduction

This work is an extended version of the paper [1] initially presented at the 16th Iberian Conference on Information Systems and Technologies (CISTI 2021).

Requirements Engineering (RE) has come a long way and is currently considered a set of good practices for pragmatic, results-focused critical thinking - applicable to any domain [2]. Agile development processes have also come to promote flexibility and adaptability in the face of inevitable changes in requirements, producing software in small increments and getting feedback in rapid iterations [3]. Recent studies [4] have identified that approaches that use creativity in requirements elicitation can be successfully implemented in real software projects. The possibility of using known creativity techniques, or adaptations, to mediate idea generation, help produce new combinations, and provide unexpected, original, practical, and satisfying answers in software development seems challenging.

This paper proposes an approach, CRESustain, for incorporating creativity and sustainability in the RE process, aiming at building more agile and sustainable software, which consequently allows for greater competitiveness and longevity. This paper also proposes integrating sustainability factors when introducing creativity in RE to overcome the barriers to incorporating sustainability in the RE process. The research works of [5] reinforce the need to incorporate creativity in the RE process. By looking at sustainability concerns, it is possible to incorporate guidelines into the requirements specification stages.

The paper is structured in six sections. The first section introduces the problem; the second presents the methodology used in the research; section three presents creativity and sustainability in RE; the proposed approach for incorporating sustainability and creativity factors in RE is presented in section four; section five describes the application of the approach; finally, in section six, the conclusions and perspectives for future work are discussed.

## 2. Methodology supporting the work

Based on the specificity of the subject under investigation, the Design Science Research Methodology (DSRM) was adopted to obtain scientific support for the study [6] that led to the design of the artefact - the CRESustain approach. The DSR process typically includes six steps or activities, illustrated in Figure 1. In selecting the methodology, the types of practical applications were also considered [7]. In this case, the focus is on applicable artefact development.,

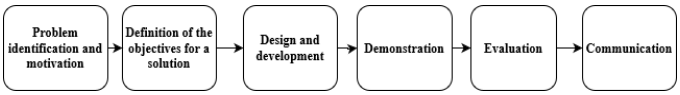


Figure 1: Design Science Research Methodology activities (adapted from [6])

The DSRM is a powerful tool for improving methods in engineering education research and provides specific guidelines for evaluation and iteration within research projects. DSRM focuses on artefact development with the explicit intention of improving the functional performance of the artefact [8]. In this context, it is considered that, given the specificity of the research under study, the DSRM allows the necessary iterations to identify the problem, define objectives, design, develop, demonstrate, evaluate, and communicate the artefact.

## 3. Background

Requirements Engineering [5] is the engineering discipline that includes all requirements definition and specification activities. RE concerns software systems' goals, functionalities, and constraints [9].

### *3.1. Creativity*

Introducing creativity into the RE process seems to have enormous potential. The discussion about the potential of creativity in RE has been studied [10]; [11]; [12]. The importance of creative and heuristic techniques in solving engineering problems is recognized [13]. Problem-solving largely depends on innovation, creativity, intuitive design, correct analysis, and effective project management. In addition, experience from previous projects helps professionals in the early stages of identifying ideas [14].

Research into how the application of creativity occurs in RE has been neglected [13], [15]. Applying creative techniques will allow requirements engineers to work on problems, areas, and contexts with a combination of existing methods and techniques.

The scientific community has given importance to the incorporation of creativity in RE education [10] [16] [17]. Creativity workshops have been continuously held at major RE conferences such as the International Requirements Engineering Conference and the Australian Workshop on Requirements Engineering.

The authors [18] refer to the importance of creativity during the requirements analysis phase. They suggest that several creativity techniques, such as brainstorming, scenarios, and simulations, can be used to promote creativity during this phase.

### *3.2. Sustainability*

Sustainability assumes increasing importance. The concept of sustainability in Requirements Engineering has been analyzed and discussed at the International Workshop on Requirements Engineering for Sustainable Systems. In the same direction, the Karlskrona Manifesto has given excellent visibility to the concept of sustainability design [19]. This Manifesto contains sustainability guidelines for the design of software systems. In this context and to help with this sustainability task, the Karlskrona Manifesto proposes nine principles (Figure 2) and commitments.

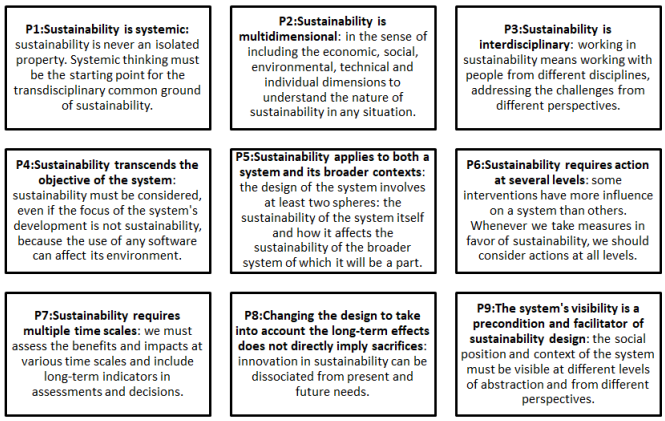


Figure 2: Principles of the Karlskrona Manifesto

One of the current challenges is the lack of practical examples that show the use of Karlskrona Manifesto principles during requirements gathering [20] and software design.

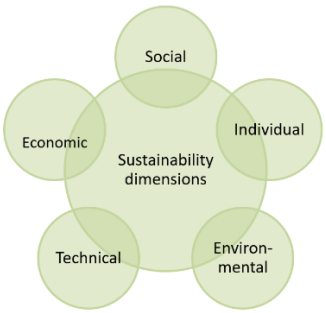


Figure 3: The five dimensions of sustainability

The Karlskrona Manifesto [21] argues that sustainability should be analyzed in five dimensions (Figure 3). The dimensions of Figure 3 are interconnected, providing a tool to analyze relevant sustainability issues for society [22]. In this sense, principle P2, "Sustainability is multidimensional," of the Karlskrona Manifesto

encourages the different dimensions of sustainability to be integrated into the RE process.

Since requirements define how and what a piece of software will do, the authors [21] argue that requirements engineering is the critical point in software engineering through which sustainability can be promoted. The introduction of sustainability during the RE process allows us to analyze the achievability of promoting and incorporating the United Nations' 17 Sustainable Development Goals (SDG) [23]. In fact, for the authors [24], sustainability is one of the pillars of software development.

According to [25], creativity is a fundamental element of sustainable development. In [26] perspective, the relationship between sustainability and creativity is very close, highlighting the need to place creativity as a resource at the center of sustainability. That is a renewable resource at the service of problem-solving.

In the authors' perspective, [20], [21], [27], [28], the need to include sustainability in RE is recognized. Research results from [29] indicate the importance of considering both technical and non-technical aspects of sustainability; putting one in contention and ignoring the other will threaten software products' sustainability [30]. The results of the study [31] on how to raise awareness of the potential effects of software systems on sustainability indicate that the application of the SuSAF framework facilitates the discussion in terms of sustainability. This framework is intended to be used by requirements engineers to facilitate stakeholder engagement.

However, none of the cited approaches focused on applying creativity techniques to incorporate sustainability principles and dimensions during the RE process. The gaps found in the literature are centered on incorporating sustainability by applying creative processes during requirements specifications.

## 4. Approach to Sustainability and Creativity in Requirements Engineering - CRESustain

This section presents a strategy for incorporating sustainability factors when introducing creative techniques into RE and an approach to operationalizing it.

It is often assumed that the creative process that can be useful for RE is complex. It would be advantageous to have a structured approach that is powerful enough to generate results and flexible enough to be used and adjusted to any RE approach that includes sustainability. These considerations justified the creation of an approach, CRESustain, for introducing sustainability and creative processes in RE.

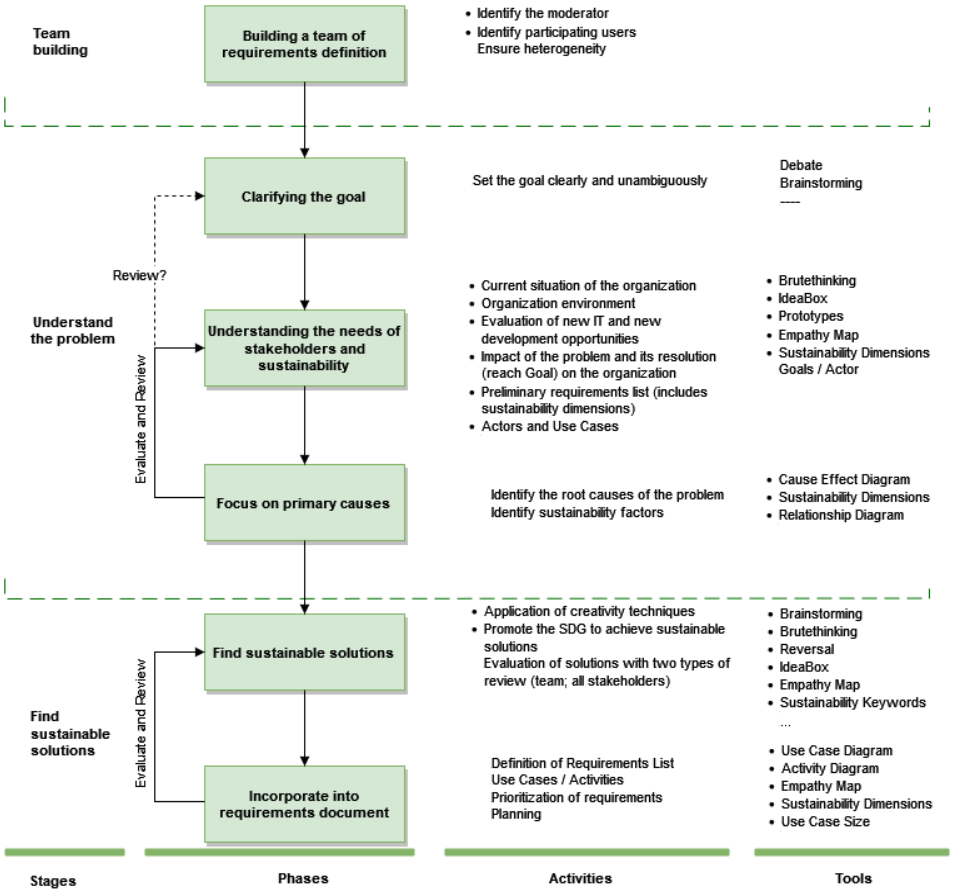


Figure 4: Approach to incorporating sustainability and creativity into RE - CRESustain

CRESustain, shown in Figure 4, is within the context of a more comprehensive methodology [1], [32], [33], [34]. It uses various creativity techniques considered appropriate for different activities and based on existing methods and techniques for creative problem solving, in particular the Creative Problem-Solving Process [35] and the Productive Thinking Model [36]. It incorporates the dimensions of sustainability and the principles of the Karlskrona Manifesto [19], in that requirements engineering is the crucial phase to promote sustainability.

As shown in Figure 4, the approach includes three stages: team building, understanding the problem, and finding sustainable solutions; and six linked phases indicating the flow of information between the steps. The first phase aims to set up a team that will apply the approach called "Building a team of requirements definition." Each phase contains several activities with supporting tools.

In phase 2, "Clarifying the goal," the formulation of a concrete goal is sought. The problem statement helps think about the general first and then the specific problem. In other words, it provides a structure for identifying the objectives that help to solve the problem. For this activity, "Clarify the goal," the Brainstorming technique is used to generate ideas without restrictions [32].

Phase 3, "Understanding the needs of stakeholders and sustainability," involves gathering requirements involving users/stakeholders in a spiral process to find creative solutions to achieve sustainability. Similar applications are used as prototypes to analyze and validate software requirements. In this step, empathy maps [37] help identify and understand the scenario where the end user is inserted, their vision, limitations, needs, and desires. The preliminary list of requirements is prepared, with actors and their objectives in a Use Case format [3]. The activity for analyzing prototypes by applying the IdeaBox creativity technique is also worth mentioning. This technique allows the combination of a challenge's parameters (characteristics, factors, variables, or aspects) into new ideas [32]. From this phase, the 17 SDGs and the five dimensions of sustainability are integrated.

In the "Focus on primary causes" phase, the root causes at the problem's origin are identified and highlighted. For effect, the elaboration of cause-effect diagrams and relationship diagrams is proposed; the sustainability factors are also identified, and the nine principles of the Karlskrona Manifesto [19] were incorporated. During the ER process, abstraction is used to manage the complexity of the problem and apply the Manifesto's nine principles.

The incorporation of sustainability factors takes place through the analysis of the five dimensions of sustainability: human, environmental, social, technical, and economic. These sustainability dimensions are incorporated in the Karlskrona Manifesto [19] to address sustainability concerns in several areas, namely:

- Human/Individual Sustainability: concerns the maintenance of human capital (e.g., education, health, skills, knowledge, leadership, and access to services);
- Economic sustainability: aims to maintain capital and value-added;
- Environmental sustainability: refers to improving human well-being by protecting nature and its resources, such as water, earth, minerals, air, and ecosystem services;
- Technical sustainability: about the longevity of information, systems, and infrastructure and their adequacy to changing environmental conditions;
- Social Sustainability: aims to preserve social communities in solidarity and services.

In this phase, "Focus on primary causes," it is important to reflect on the Relationship Diagram of the principles of the Karlskrona Manifesto and the SDG.

Phase 5, "Finding sustainable solutions," is aimed at building and evaluating solutions considering the objective, the organization's needs, and sustainability factors, given the specificity of the business. Different creativity techniques are applied to obtain innovative solutions that address the primary causes and the five dimensions of sustainability. Thus, the creativity techniques proposed for this stage are Brutethinking and Reversal [32]. After applying the creative techniques, the sustainability keyword diagram is developed based on the human, environmental, social, technical, and economic dimensions, focusing on the SDG and people's needs. The empathy map is helpful during the validation of ideas.

The iterative process of CRESustain ends with phase 6, "Incorporate into the requirements document," whose purpose is to bring together all the elements of the process, namely: the documentation that results from the application domain information (phase 3); the list of requirements and supporting diagrams; the specific information with the requirements priorities (comprises the interaction with stakeholders to discover the most critical requirements); the empathy maps, to synthesize and organize the discussed contents; eventual prototypes of the system; the risk assessment and a project map.

The approach proposes validating requirements at two levels: within the team and in a general meeting with stakeholders. In other words, it corresponds to the TwoTierReview pattern [38], in which the full group should perform the review at least once.

It has already been possible to apply the approach in an academic context and a real-life context in a social organization.

## 5. Evaluation

A social organization providing services to a local community was selected to identify requirements that constitute added value in sustainability to evaluate the approach's applicability. A multidisciplinary team assessed the approach in a social organization. The social organization consists of a social center called São Domingos, which supports a Community (SDC).

The first phase, "Building a team of requirements definition," included elements from several areas, namely: the Project Manager with experience in information systems optimization; a Requirements Engineer with experience in the ER process; a Software Architect with development experience; and the Manager of the SDC (as end-user). The team also collaborated with the specialist engineer in applying creativity techniques to validate the approach.

After characterizing the community (in terms of gaps and opportunities for improvement), the team followed the steps underlying the process, namely: clarification of the goal, understanding of the needs of stakeholders and sustainability factors, focusing on primary causes, finding sustainable solutions and integrating into the requirements document.

It should be noted that to "Find sustainable solutions," the needs of the organization and the primary causes were considered, applying different creativity techniques to obtain innovative and sustainable solutions. At this point, we proceeded to select the most appropriate creative techniques given the specificity of the organization under study. Brutethinking and Reversal techniques were selected. Empathy maps were used to synthesize and organize the selected contents and ideas.

During the application of the Brutethinking creativity technique, the word sustainability associated with the problem was introduced. After analyzing the ideas obtained, the following SDGs were included (3 - Good Health and Well-being; 4 - Quality Education; 8 - Decent Work and Economic Growth; 9 - Industry, Innovation, and Infrastructure; 17 - Partnerships for the Goals) and the five dimensions of sustainability: human, economic, environmental, technical, and social.

The creative process was repeated to reflect and identify the connections between the five dimensions of sustainability. In this way, Figure 5 was created to present the result of this reflection in a diagram with keywords in the five dimensions of sustainability in the SDC. According to the representation in Figure 5, it was possible to obtain the integration of the five dimensions of sustainability because of the reflection of the real situation of the social organization.

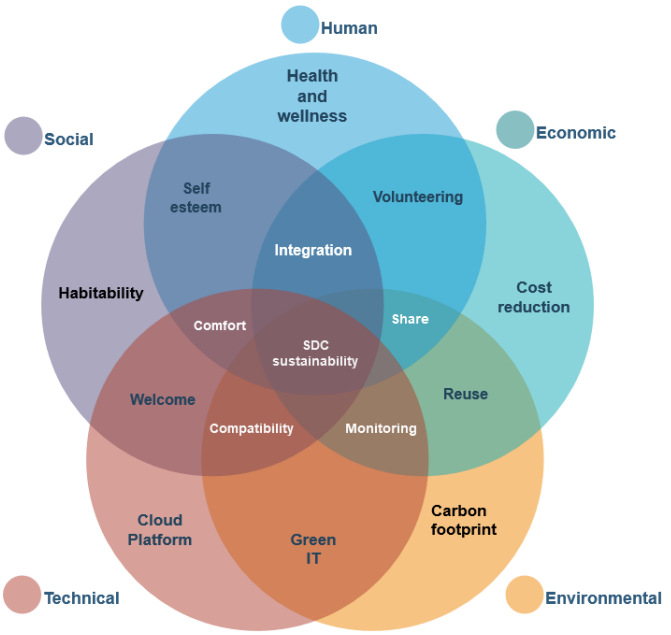


Figure 5: Sustainability dimensions in SDC

The main results focus on the visualization of the five dimensions of sustainability applied to the social organization under study. In this context, sustainability, particularly Sustainable Development Goal 17, encouraged the creation of partnerships to solve social problems. It should also be noted that the team was given sufficient guidance so that the actions do not seem mysterious, leaving room for innovation and participation.

The CRESustain approach was also applied in an academic context with a group of students in a Software Engineering course. The results underlying the interaction with students showed difficulties in relating the dimensions of sustainability to academic projects, namely the ability to visualize the benefits of the SDG after project implementation. On the other hand, it was observed that it is necessary to understand the concept of sustainability and its interconnection with software engineering.

Overall, it is concluded that creativity techniques were applied correctly, having achieved the objective of developing sustainable innovations in ongoing projects. It was possible to include sustainability factors in the creative approach by associating the five dimensions of sustainability and integrating the SDG.

The principles and commitments of the Karlskrona Manifesto are considered in applying the approach to provide a comprehensive view of sustainability and opportunities encouraging various stakeholders to include sustainable solutions during the RE process.

It is essential to mention that the sustainability factors incorporated in the RE process can be applied to other software products, referring to the following examples: smart home systems, washing machines or games [27]; digital signature of documents [22]; a platform for homeless people [40]; mobile applications for volunteering and insulin monitoring in diabetics [41]; taking medication [42]; agricultural land for cultivation [43].

## 6. Conclusion

The paper's innovative contribution concerns incorporating sustainability principles and dimensions with creativity techniques during the RE process, creating a CRESustain approach. Applying the specific structured CRESustain approach to introduce sustainability concepts and creative processes in RE focuses on three main stages: team building, understanding the problem and finding sustainable solutions. The word sustainability is introduced during the creative process by building the respective diagram and identifying sustainable solutions in its five dimensions: human/individual, economic, environmental, technical, and social. The study observed that this approach stimulates discussion about sustainability in its multiple dimensions, promotes the SDG, and focuses on people's needs.

The practical application of the CRESustain approach showed that it was possible to identify sustainability requirements that led to creating new services in the social organization. Another result obtained was the interconnection of the identified requirements to the SDG.

The difficulties were focused on the introduction of creativity techniques and sustainability dimensions. This difficulty was solved by training the whole team.

It is reiterated that innovation, creativity, and sustainability at the technical/non-technical and/or functional level are essential factors for the success of software products. Thus, the participation of elements with skills in these areas is also fundamental, allowing a reflection on the requirements and their effects on sustainability.

It is also observed that software professionals have shown interest in the sustainability issue, and there is a certain consensus that sustainability should be treated as a software quality attribute. Considering sustainability as an attribute of software quality allows incorporating the principles and commitments of the Karlskrona Manifesto and emphasizing the five dimensions of sustainability: individual/human, social, environmental, technical, and economical. The DSR methodology, applied in an iterative process, allowed the design of the artefact.

The study's limitations were at the level of surveying sustainability requirements to meet the principles of the Karlskrona Manifesto and thus contribute to promoting the SDG. The fact that it was only applied to a social project is also considered another limitation.

In future work, it is planned to continue the application of the approach in academic co-creation projects. Another operational perspective that can provide added value to extend the approach will be to analyze the organization's representation by its DNA and use the enterprise architecture structure for this purpose [44].

## Conflict of Interest

The authors declare no conflict of interest.

## References

[1] C. Silveira, V. Santos, L. Reis, H. Mamede, "A new Approach to Sustainability and Creativity in Requirements Engineering," *16th Iberian Conference on Information Systems and Technologies (CISTI)*, pp. 1–6, 2021, doi:10.23919/CISTI52073.2021.9476532.

[2] D. Callele, K. Wnuk, B. Penzenstadler, "New Frontiers for Requirements Engineering," *IEEE 25th International Requirements Engineering Conference (RE),* pp. 184-193, 2017, doi: 10.1109/RE.2017.23.

[3] I. Jacobson, H. Lawson, P.-W. Ng, P. E. McMahon, M. Goedicke, *The Essentials of Modern Software Engineering: Free the Practices from the Method Prisons*, ACM Books, 2019.

[4] A. Aldave, J. Vara, D. Granada, E. Marcos, "Leveraging creativity in requirements elicitation within agile software development: A systematic literature review," *Journal of Systems and Software,* vol. 157:110396, 2019, doi:10.1016/j.jss.2019.110396.

[5] S. Thew, A. Sutcliffe, "Value-based requirements engineering: method and experience," *Requirements Engineering,* vol. 23, pp. 443–464, 2018, doi:10.1007/s00766-017-0273-y.

[6] K. Peffers, T. Tuunanen, M. Rothenberger, S. Chatterjee, "A Design Science Research Methodology for Information Systems Research," *Journal of Management Information Systems,* vol. 3, no. 24, pp. 45-78, 2007, doi: 10.2753/MIS0742-1222240302.

[7] K. Peffers, T. Tuunanen, B. Niehaves, "Design science research genres: introduction to the special issue on exemplars and criteria for applicable design science research," *European Journal of Information Systems, 27:2,* pp. 129-139, 2018, doi: 10.1080/0960085X.2018.1458066.

[8] K. Carstensen, J. Bernhard, "Design science research – a powerful tool for improving methods in engineering education research," *European Journal of Engineering Education,* vol. 44, no. 1–2, pp. 85–102, 2019, doi: 10.1080/03043797.2018.1498459.

[9] P. Loucopoulos, E. Kavakli, J. Mascolo, "Requirements Engineering for Cyber Physical Production Systems: The e-CORE approach and its application," *Information Systems,* vol. 104, 2022, doi:10.1016/j.is.2020.101677.

[10] T. Bhowmik, "Creativity in Requirements Engineering: Why and How?," *IEEE Software Blog,* 2016.

[11] M. Mahaux, L. Nguyen, l. Mich, A. Mavin, "A framework for understanding collaborative creativity in requirements engineering: Empirical validation," *4th Int. Work. on Empirical Requirements Engineering (EmpiRE)*, pp. 48-55, 2014, doi: 10.1109/EmpiRE.2014.6890116.

[12] N. Maiden, S. Jones, K. Karlsen, R. Neill, K. Zachos, A. Milne, "Requirements engineering as creative problem solving: A research agenda for idea finding," *International Requirements Engineering Conference*, pp. 57-66, 2010, doi: 10.1109/RE.2010.16.

[13] O. Hoffmann, D. Cropley, A. Cropley, L. Nguyen, P. Swatman, "Creativity, Requirements and Perspectives," *AJIS,* vol. 13, no.1, 2005, doi: 10.3127/ajis.v13i1.69.

[14] R. Hegde, G. S. Walia, "How to Enhance the Creativity of Software Developers: A Systematic Literature Review," *International Conference on Software Engineering and Knowledge Engineering, SEKE 2014*, pp. 229-234, 2014.

[15] R. Mohanani, P. Ram, A. Lasisi, P. R. a. B. Turhan, "Perceptions of Creativity in Software Engineering Research and Practice," *43rd Euromicro Conference on Software Engineering and Advanced Applications (SEAA),* pp. 210-217, 2017, doi: 10.1109/SEAA.2017.21.

[16] T. Bhowmik, N. Niu, A. Mahmoud, J. Savolainen, "Automated Support for Combinational Creativity in Requirements Engineering," *International Requirements Engineering Conference (RE)*, pp. 243-252, 2014, doi: 10.1109/RE.2014.6912266.

[17] L. Nguyen, G. Shanks, "A framework for understanding creativity in requirements engineering," *Information and Software Technology*, vol. 51, no.3, p. 655–662, 2009, doi: 10.1016/j.infsof.2008.09.002.

[18] L. Nguyen, P. Swatman, "Promoting and Supporting Requirements Engineering Creativity," *Rationale Management in Software Engineering,* pp. 209-230, 2006, doi: 10.1007/978-3-540-30998-7_10.

[19] C. Becker, R. Chitchyan, L. Duboc, S. Easterbrook, B. Penzenstadler, N. Seyff, C. Venters, "Sustainability Design and Software: The Karlskrona Manifesto," *Proc. 37th International Conference on Software Engineering (ICSE 15)*, pp. 467-476, 2015, doi: 10.1109/ICSE.2015.179.

[20] S. Oyedeji, B. Penzenstadler, "Experiences from Applying the Karlskrona Manifesto Principles for Sustainability in Software System Design," *Proceedings of the 8th International Workshop on Requirements Engineering for Sustainable Systems,* 2020.

[21] C. Becker, S. Betz, R. Chitchyan, L. E. S. Duboc, B. Penzenstadler, N. Seyff, C. Venters, "Requirements: The Key to Sustainability," *IEEE Software,* vol. 33, no. 1, pp. 56-65, 2016, doi: 10.1109/MS.2015.158.

[22] B. Ovelheiro, C. Silveira, L. Reis, "Sustainability Design Applied to the Digital Signature of Documents," *Handbook of Research on Multidisciplinary Approaches to Entrepreneurship, Innovation, and ICTs*, IGI Global, pp. 349-374, 2021, doi:10.4018/978-1-7998-4099-2.ch016.

[23] United Nations Development Programme, "Sustainable Development Goals," 2015. [Online]. Available: www.undp.org/content/undp/en/home/sustainable-development-goals.html. [Accessed 02 12 2019].

[24] J. Cohen, D. S. Katz, M. Barker, N. C. Hong, R. Haines, C. Jay, "The Four Pillars of Research Software Engineering," *IEEE Software,* vol. 38, no. 1, pp. 97-105, 2021, doi:10.1109/MS.2020.2973362.

[25] A. M. Kanzola, P. E. Petrakis, "The Sustainability of Creativity," *Sustainability,* vol. 13, no. 5, 2776, 2021, doi: 10.3390/su13052776.

[26] H. d'Orville, "The relationship between sustainability and creativity," *Cadmus,* vol. 4, no. 1, pp. 65-73, 2019.

[27] S. Oyedeji, A. Seffah, B. Penzenstadler, "A Catalogue Supporting Software Sustainability Design," *Sustainability,* vol. 10, no. 7, 2296, 2018, doi: 10.3390/su10072296.

[28] K. Roher, D. Richardson, "Sustainability requirement patterns," *3rd International Workshop on Requirements Patterns (RePa)*, pp. 8-11, 2013, doi: 10.1109/RePa.2013.6602665.

[29] A. Imran, T. Kosar, "Software Sustainability: A Systematic Literature Review and Comprehensive Analysis," *rXiv preprint arXiv:1910.06109*, 2019.

[30] A. Fonseca, R. Kazman, P. Lago, "A manifesto for energy-aware software," *IEEE Software,* vol. 36, no. 6, pp. 79-82, 2019, doi: 10.1109/MS.2019.2924498.

[31] L. Duboc, B. Penzenstadler, J. Porras, S. Akinli Kocak, S. Betz, R. Chitchyan, C. C. Venters, "Requirements engineering for sustainability: an awareness framework for designing software systems for a better tomorrow," *Requirements Engineering,* vol. 25, no. 4, pp. 469-492, 2020, doi:10.1007/s00766-020-00336-y.

[32] V. Santos, *Criatividade em Sistemas de Informação*, Lisboa: FCA, 2018.

[33] C. Silveira, L. Reis, V. Santos, H. Mamede, "Creativity in Prototypes Design: The case of Social Organizations," *CISTI'2020 - 15th Iberian Conference on Information Systems and Technologies*, pp. 1-6, 2020, doi: 10.23919/CISTI49556.2020.9140870.

[34] V. Santos, H. Mamede, C. Silveira, L. Reis, "Methodology for Introducing Creativity in Requirements Engineering," *Procedia Computer Science Journal,* vol. 196, pp. 27-35, 2022, doi: 10.1016/j.procs.2021.11.069.

[35] A. Osborn, *Applied Imagination: Principles and Procedures of Creative Problem-Solving*, Creative Education Foundation, 1963.

[36] T. Hurson, *Think Better: An Innovator's Guide to Productive Thinking*, New York: McGraw-Hill, 2007.

[37] S. Malhotra, "Empathy Mapping | Fulfilling User Needs with Digital Designs," 2019 . [Online]. Available: https://www.oodlesstudio.com/blog/empathy-mapping-ux-ui-consulting-services/.

[38] S. Adolph, P. Bramble, *Patterns for Effective Use Cases*, Addison-WesleyPearson Education, 2003.

[39] C. Silveira, L. Reis, "Sustainability in Information and Communication Technologies," *Research Anthology on Measuring and Achieving Sustainable Development Goals*, IGI Global, pp. 771-792, 2022, doi: 10.4018/978-1-6684-3885-5.ch041.

[40] L. Reis, C. Silveira, L. Carvalho, C. Mata, "Digitalization as a Key Issue of the Circular Economy to Promote Sustainability: Prototyping Design for Homeless People," Research Anthology on Measuring and Achieving Sustainable Development Goals, IGI Global, pp. 270-296, 2022, doi: 10.4018/978-1-6684-3885-5.ch014.

[41] J. Torres, D. Julio, C. Silveira, L. Reis, "Diabetes Tracker and Volunteer+ Software Engineering for Sustainability," *Digitalization as a Driver for Smart Economy in the Post-COVID-19 Era*, IGI Global, pp. 198-227, 2022, doi: 10.4018/978-1-7998-9227-4.ch011.

[42] Design Sustainability, "Cognatio – Medication Adherence," *The Karlskrona Manifesto for Sustainability Design*, 2021. [Online]. Available: https://www.sustainabilitydesign.org/2015/08/28/cognatio-medication-adherence/. [Accessed 20 01 2021].

[43] C. Silveira, L. Reis, L. Carvalho, C. Tomé, P. Sanches, "Sustentabilidade Multidimensional na promoção da Igualdade de Género na Ciência/Tecnologia," *Innovative Driving Marketing for a Better World. The Emergence of Social Proposals in Pandemic Times*, pp. 119-125, 2021.

[44] R. Trotsyuk, V. Santos, "The Enterprise DNA: Static and Dynamic Digital Representation of Organizations," *International Journal of Engineering and Advanced Technology,* vol. 8, no. 6, pp. 5034-5038, 2019, doi: 10.35940/ijeat.B5552.088619.



**Clara Silveira**: Coordinator Professor at the School of Technology and Management (ESTG) of the Polytechnic of Guarda. Teaching activities, since 1991, in the field of "Software Engineering and Information Systems" to the Computer Science Engineering degree and the MSc in Mobile Computing.

She holds a PhD in Electrical and Computer Engineering from the Faculty of Engineering, University of Porto (FEUP); Master in Electrical and Computer Engineering, specializing in Industrial Informatics at FEUP; and completed the Training Program on Public Management (FORGEP) by INA. Director of the Software Engineering and Information Systems field. She has eight years of experience leading the ESTG management team.

**Leonilde Reis**: Coordinator Professor with Aggregation at the School of Business and Administration (ESCE) of the Polytechnic Institute of Setúbal (IPS). The activities of teaching in higher education were developed since 1992 in the field of "Information Systems" and focused on undergraduate, master's and doctoral courses.
Aggregation in Information Sciences, Fernando Pessoa University; PhD in Systems Information and Technologies, Minho University; Master's in management informatics, Católica University. Author of several publications in national and international journals, books and book chapters.

**Vitor Santos**: Assistant Professor at NOVA IMS. Holds a PhD in Technology information Systems Science from University of Minho. A Degree in Informatics Engineering from Cocite, a Postgraduate course in Computer Science from Science Faculty of Lisbon University, a M.Sc. and a DEA in information Systems
Science from Minho University and a Computer Specialist title from polytechnic institutes Guarda, Castelo Branco and Viseu. Integrates several national and international conferences scientific committees and has authored several academic publications (~150) (>40 IS projects). Was an elected member of the Order of Engineers and of APDSI board.

**Henrique Mamede**: Assistant Professor at Department of Sciences and Technology of Universidade Aberta (Portuguese Open University). Invited professor at NOVA IMS. Senior researcher at INESC TEC. Habilitation in Web Science and Technology.
Holds a PhD in Information Systems and Technologies from University of Minho. An MSc in Informatics from Lisbon University. A degree in Informatics Engineering from COCITE. A PostGraduate course in Information Management from Portuguese Catholic University. Integrates several national and international conferences scientific committees and has authored several academic publications.